

A New Perspective on the Scalar Meson Puzzle, from Spontaneous Chiral Symmetry Breaking Beyond BCS

Pedro J. de A. Bicudo

Departamento de Física and Centro de Física das Interações Fundamentais, Edifício Ciência, Instituto Superior Técnico, Av. Rovisco Pais, 1096 Lisboa, Portugal

We introduce coupled channels of Bethe-Salpeter mesons both in the mass gap equation for chiral symmetry breaking and in the boundstate equation for mesons. Consistency is insured by the Ward Identities for axial currents, which preserve the Goldstone boson nature of the pion. We find that the coupling of channels yields the widths of resonances and contributes to mass splittings, but it does not shift globally the hadron spectrum. We find that coupled channels reduce the breaking of chiral symmetry. This reduction is constrained by the coupling of a scalar meson to a pair of pseudoscalar mesons. The light and wide $\sigma - f_0(600)$, the narrow $f_0(980)$ and the relatively heavy $f_0(1370)$ are studied in order to comply with the spontaneous breaking of chiral symmetry. Exact calculations are performed in a particular model. In this model we find that the $f_0(980)$ is the best candidate for the groundstate quark antiquark meson. In particular its width is naturally small. In this case the coupled channels reduce strongly the breaking of chiral symmetry.

12.39.Kc, 11.30.Rd, 14.40.Cs, 13.25.Jx

I. INTRODUCTION

The Scalar puzzle

The scalar mesons form perhaps the most puzzling family in hadronic physics. The first puzzling fact concerns the decay widths Γ of the scalars f_0 and a_0 into pseudoscalar pairs in an S-wave. This would naively be expected to be much larger than the decay widths of resonances decaying in pseudoscalar pairs with higher angular momentum, for instance the ρ which decays in p-wave pseudoscalar pairs. This is not the case for the flavor vectors and we find [1] that $\Gamma_{a_0(980)} \simeq 0.3 \rightarrow 0.6 \Gamma_{\rho(770)}$. The second puzzling argument concerns the excess of states from the point of view of simple $q\bar{q}$ states. The One Meson Exchange Potential models for the NN interaction favor a scalar meson sometimes known as σ with $M \simeq 0.5 \text{ GeV}$. The scalar σ would provide most of the intermediate range attraction. A meson with a similar mass of $400 - 1000 \text{ MeV}$ (but with a very large width of $600 - 1000 \text{ MeV}$) would also reproduce the low momentum $\pi\pi$ scattering. But if one would add this unconfirmed state to the well established ones, see Fig. 1, then an excess of states would exist. It is also puzzling that the decay widths of the $f_0(980)$ and $a_0(980)$ are not precisely determined. The highest experimental bound on these Γ

was of the order of $40 - 50 \text{ MeV}$ before 1992, in 1994 it jumped to $400 - 300 \text{ MeV}$ and dropped to 100 MeV in 1996. This is quite uncommon in the Review of Particle Properties [1].

The puzzling phenomena involving the light scalar meson family has drawn a wealth of theoretical interpretations. The model of Isgur and Weinstein et al [2] finds that the narrow scalars are meson-meson molecules which would then be the excess non $q\bar{q}$ states. It is also advocated that the excess states could be glueballs [3]. The most economical models include just mesons which are strongly coupled, and can perhaps be derived from quark models. These models can be tuned [4,5] to explain with complex nonlinear effects not only the narrow resonances which are due to the vicinity of the KK threshold, but also the very wide and light $f_0(600)$ which would appear as an extra pole in the S matrix when couplings are large.

We propose here a new perspective to the scalar meson puzzle. Unlike the vector, axial and tensor mesons, the scalar and pseudoscalar mesons are mixed by the chiral rotations,

$$\begin{aligned}\bar{\psi}\psi &\rightarrow \cos(\theta)\bar{\psi}\psi + i\sin(\theta)\bar{\psi}\gamma_5\psi \\ \bar{\psi}\gamma_5\psi &\rightarrow -i\sin(\theta)\bar{\psi}\psi + \cos(\theta)\bar{\psi}\gamma_5\psi,\end{aligned}\quad (1)$$

moreover the chiral condensate is generated from the trivial vacuum by scalars, which consist [6] of 3P_0 quark antiquark pairs. thus we expect that not only the pseudoscalar mesons but also the scalars must contain the signature of the breaking of chiral symmetry.

Chiral Symmetry Breaking at the BCS level

Dynamical Spontaneous Chiral Symmetry Breaking (χSB) has been worked out in the past with several different quark-quark effective interactions, at the same level as Bardeen Cooper and Schrieffer (BCS) did [7] for Superconductivity. For instance, a strong or a confining chiral invariant quark-quark interaction suffices to condense in the vacuum scalar quark-antiquark pairs, inducing dynamical chiral symmetry breaking.

However since Nambu and Jona-Lasinio (NJL) and until recently [9,10] the mass gap equation in chiral physics has been so far of the BCS type, [8] including only the first order contribution from the quark-quark interaction. For instance with a color dependent interaction the Schwinger Dyson mass gap equation is,

$$\begin{aligned} \text{---} \text{---}^{-1} &= \mathcal{S}_0^{-1} - \text{---} \text{---} \text{---} \\ \mathcal{S}^{-1} &= -i \not{p} - \Sigma \end{aligned} \quad (2)$$

We shall call this approximation the BCS level, although the coupling is strong. For a perturbative departure from the BCS approximation, see [9] The full (up to the approximation which is chosen) propagator \mathcal{S} is denoted as usual by --- and the full vertex Γ^μ will be denoted by $\bullet\text{---}$. Here we follow the normal notation Γ^μ for the vertex, which should not be confused with a similar notation Γ for the decay width of resonances. The subindex $_0$ is reserved for the free fields. The effective quark-quark 2-body interaction, a chiral invariant and color dependent interaction, is represented with a dotted line \cdots . See for instance eq. (17). In the NJL and until recently [9,10], the bound state equation was only solved at the ladder level, and not all quartic interactions were included. For instance the Bethe Salpeter equation for the vertex is,

$$\bullet\text{---} = \Gamma_0 + \text{---} \text{---} \text{---} \bullet\text{---} \quad (3)$$

In particular the diagrams leading to coupled channels with the creation or annihilation of a quark-antiquark color singlet pair were not used, see for instance Fig. 2. Thus at the BCS level of chiral symmetry breaking, the quark models have no resonances, and have just boundstates with real poles (except for the decay into free quarks in the case of nonconfining models). The mesonic coupled channels are described microscopically with the BS ladder which will be represented diagrammatically by a box with 4 emerging lines \square . We get for instance,

$$\begin{aligned} \text{---} \square \text{---} &= \text{---} \text{---} + \text{---} \text{---} \text{---} + \text{---} \text{---} \text{---} \text{---} + \dots \\ &= \sum_b \text{---} \triangle_b \text{---} \end{aligned} \quad (4)$$

where b represents the quark-antiquark boundstates. In the case of an effective confining potential, there are no continuum quark-antiquark states and only color singlet boundstates exist. The quark antiquark BS amplitude is represented by the triangle \triangle and the boson propagator of the meson is represented by the double line \equiv . For instance the dressed vertex which is obtained with the iteration of eq. (3) includes this ladder. The ladder itself is bare in the sense that it does not include coupled channels of mesons.

Coupled Channels of Mesons

In the case of weak coupled channel effects, it would be acceptable to couple the boundstates obtained at the BCS level with the diagrams of Fig. 2, without changing the mass gap equation. In this sense we started some

years ago to develop a program [11] to study the coupled channel effects of quark models with chiral symmetry breaking. This work tries to retain the advantages of both NJL quark models and quark models with coupled channels. NJL models verify all the properties of Partially Conserved Axial Currents, including the pion small mass. They are also able to set with one or two parameters both the scale of the quark condensates, the hadron masses and sizes but not the width of resonances or phase shifts. Coupled channel quark models are able to study strong interactions and decays but have many parameters, for instance to set the quark masses, the confining potential, a global mass shift of boundstates, the tensor potentials, and the annihilation second quantized potentials. They also fail usually to get the low mass of the pion.

The first result of our program was to reproduce [11] at the BCS level the strong decay of the vector meson ρ (and of the Φ). This has been studied by other authors recently [12]. Later we extended our program to the nucleon interactions and had good results [11] in the K_N s-wave scattering, the $F_{N\pi N}$ and $F_{N\pi\Delta}$ derivative couplings and the NN short range interaction.

However we also found [11] that the ρ would suffer a large real mass shift, comparable to its physical mass, due to the coupling to a pair of π . This would indicate that the coupled channel effects can not be neglected in the mass gap equation. We are further motivated with the recent trend in the literature to reevaluate coupled channel effects in many hadronic phenomena. Some years ago they were not supposed to account for more than 10% of a hadron mass but presently they are supposed to contribute with a negative mass shift of the order of 50% of the bare mass [13–15].

The π problem and Ward Identities

In the pion mass we have a formal problem raised by coupled channels [10]. Suppose that the mass gap equation for chiral symmetry breaking was solved at the BCS level, i.e. without including the coupled channels, then a bare pion with vanishing bare mass would be found. If the coupled channels were then included, at posteriori, in the bound state equation then the pion mass would be the sum of the small bare mass plus a negative mass shift and thus would have a resulting negative mass, which means that the BCS vacuum is not stable when meson channels are coupled. This result is unavoidable, and can be proved variationally. It is then interesting to study whether the BCS vacuum is then close or far from the minimum energy vacuum. Moreover in the literature only a few coupled channels are usually included, and it remains to be proved theoretically that the total mass shift due to the infinite series of coupled channels is finite.

The solution to the pion mass problem is found using

[16,17] the Ward identities (WI) in order to insure that the bound state equation for the pion -a Bethe Salpeter equation with coupled channels- is consistent with the non linear mass gap equation. The WI were first derived for fermion-gauge field theories, and were initially based on the simple observation that for free fermions with propagator $\mathcal{S}_f(p) = \frac{i}{\not{p} - m}$ and a free vector vertex $\Gamma_f^\mu = \gamma^\mu$,

$$i(p_\mu - p'_\mu)\mathcal{S}(p)\Gamma^\mu(p, p')\mathcal{S}(p') = \mathcal{S}(p) - \mathcal{S}(p') \quad (5)$$

These identities are a very important tool to deduce equations for the propagator from equations for the vertex and vice-versa. The difference in the right member of the equation extends the identity to renormalized propagators and vertices. There is also a WI identity for the free axial vector vertex $\Gamma_f^{\mu 5} = \gamma^\mu \gamma^5$ that involves the free pseudoscalar vertex $\Gamma_f^5 = \gamma^5$,

$$\begin{aligned} & -i(p_\mu - p'_\mu)\mathcal{S}(p)\Gamma^{\mu 5}(p, p')\mathcal{S}(p') \\ & + 2im\mathcal{S}(p)\Gamma^5(p, p')\mathcal{S}(p') = \mathcal{S}(p)\gamma^5 + \gamma^5\mathcal{S}(p') \end{aligned} \quad (6)$$

which is valid in a renormalization program providing the interaction is chiral invariant. The WI are crucial to ensure the consistency between the mass gap equation (MGE) and the Bethe-Salpeter (BS) equation. They ensure that the self energy of the MGE is obtained (without double-counting) from the BS kernel by closing the fermion line where the vertex is inserted. In fact, according to eqs. (5, 6) the vertices can be replaced by either $\mathcal{S}(p)$ or $\mathcal{S}(p')$. Some spurious diagrams where momentum would not be conserved could be thought to appear, but they all cancel and only the diagrams that depend exclusively of p or p' remain. Inversely, they also ensure that the BS kernel is obtained if one inserts the vertex in all possible propagators of the self energy. For instance this mapping is trivial at the BCS level where the mass gap equation (2) is clearly equivalent to the bound state equation (3). Let us now consider a more general case, where the fermion self energy include a fermion line consisting in a series of bare propagators $S_{\alpha_i \beta_i}(k_i + P)$. The external momentum is P and k_i is a loop momentum. The propagators can be factorized and we get,

$$\Sigma(P) = \cdots \prod_i S_{\alpha_i \beta_i}(k_i + P) . \quad (7)$$

Then the vertex Γ can be constructed if we insert a bare vertex in all possible bare propagators, and we get,

$$\begin{aligned} \Gamma^\mu(P_1 - P_2) = & \cdots \sum_j \prod_{i1 \leq j} S_{\alpha_{i1} \beta_{i1}}(k_{i1} + P_1) \\ & \gamma^\mu \prod_{i2 \geq j} S_{\alpha_{i2} \beta_{i2}}(k_{i2} + P_2) . \end{aligned} \quad (8)$$

Inversely the original self energy can be recovered if we substitute the bare vertex by the difference of propagators,

$$\begin{aligned} i(P_{1\mu} - P_{2\mu})\Gamma^\mu = & \cdots \sum_j \prod_{i1 < j} S_{\alpha_{i1} \beta_{i1}}(k_{i1} + P_1) \\ & [S_{\alpha_j \beta_j}(k_j + P_1) - S_{\alpha_j \beta_j}(k_j + P_2)] \prod_{i2 > j} S_{\alpha_{i2} \beta_{i2}}(k_{i2} + P_2) \\ & = [\Sigma(P_1) - \Sigma(P_2)] \end{aligned} \quad (9)$$

where the products which depend on both P_1 and P_2 cancel.

A key product of the WI is the proof that a pseudoscalar Goldstone boson exists when current quark masses vanish. The proof also yields the BS amplitude itself. If dynamical symmetry breaking occurs, solutions for the self-energy equation exist with finite dynamical quark masses. An equivalent equation is the extremum equation for the vacuum energy density. It can be shown that in the case of dynamical symmetry breaking the physical vacuum, i. e. the solution with the lowest energy density, is the same where the (quasi) quarks have the largest dynamical mass. We will follow a variant of NJL and Pagel's proof [8,18] to illustrate how the WI shows that the π is a Goldstone Boson when chiral symmetry is dynamically broken. The full propagator is then renormalized and the self-energy Σ has a mass-like term,

$$\mathcal{S}^{-1}(p) = \mathcal{S}_0^{-1}(p) - \Sigma(p) , \quad i\Sigma = A(p) - \not{p}B(p) . \quad (10)$$

If we substitute this propagator in the WI, we find the solution for the pseudoscalar vertex Γ^5 with a vanishing $p - p'$,

$$\Gamma^5(p = p') = \frac{A(p) + m}{m} \gamma^5 \quad (11)$$

which diverges for a vanishing quark mass m and shows that the pole of a massless pseudoscalar meson appears in the axial vector vertex, with a boundstate amplitude of

$$\chi(p - p' \simeq 0) = \frac{A\gamma_5}{f_\pi} \quad (12)$$

where f_π includes a norm. Incidentally, this identity also offers a proof of the Gell-Mann, Oakes and Renner relation. If we expand the vertex Γ^5 in the neighborhood of the π pole,

$$\Gamma^5 = \chi \frac{i}{(p - p')^2 - M^2} \chi \gamma_5 , \quad (13)$$

and substitute it in eq. (11), we find for small masses

$$\begin{aligned} m \operatorname{tr} \{ \gamma_5 \frac{A\gamma_5}{f_\pi} \} - \frac{i}{M^2} \operatorname{tr} \{ \frac{A\gamma_5}{f_\pi} \gamma_5 \} &= \operatorname{tr} \{ \gamma_5 A \gamma_5 \} \\ \Rightarrow m \int 4 A &= M^2 f_\pi^2 \quad \text{q.e.d.} \end{aligned} \quad (14)$$

In QCD it is necessary to include the axial anomaly, in the flavor singlet WI, while the flavored axial currents remain unchanged, in particular the π , K , η remain Goldstone bosons. In the flavor singlet channel of the η' , it is necessary to add $\tilde{\mathcal{F}}\mathcal{F}$ to the left member of the axial

colored state will have a mass proportional to U and will thus be confined, see eq. (57). The choice of an harmonic potential is not crucial, a linear or funnel potential has been also used, but a quadratic form is easier to use. The Fourier transform of the potential is,

$$\tilde{V}(k) = \frac{-3}{4} \frac{\tilde{\lambda}}{2} \cdot \frac{\tilde{\lambda}}{2} [-K_0^3 \nabla_k + U] (2\pi)^3 \delta^3(k). \quad (18)$$

The simpler unit system is $K_0 = 1$. and we will use it from now on. We will also work in the momentum representation and drop the tilde $\tilde{}$ from the potential.

In this case of an instantaneous interaction, it is sometimes convenient to substitute the Dirac fermions in terms of Weyl fermions. The Dirac propagator can be decomposed in a quark propagator and an antiquark propagator, moving both forward in time.

$$\begin{aligned} \mathcal{S}_{Dirac}(w, \vec{k}) &= u(k) \mathcal{S}_q(w, \vec{k}) u^\dagger(k) \beta \\ &\quad + v^\dagger(k) \mathcal{S}_{\bar{q}}(-w, -\vec{k}) v(k) \beta \end{aligned} \quad (19)$$

where the Weyl propagator is

$$\mathcal{S}_q(w, \vec{k}) = \mathcal{S}_{\bar{q}}(w, \vec{k}) = \frac{i}{w - E(k) + i\epsilon} \quad (20)$$

we choose the graphical notation for the Weyl propagators of quarks and antiquarks,

$$\mathcal{S}_q(w, \vec{k}) = \overleftarrow{\hspace{0.5cm}}_{w, \vec{k}}, \quad \mathcal{S}_{\bar{q}}(-w, -\vec{k}) = \overrightarrow{\hspace{0.5cm}}_{w, \vec{k}} \quad (21)$$

where the arrow pointing backward represents an antiquark moving forward in the time direction. With Weyl spinors the Feynman diagrams are replaced by Goldstone diagrams. The spinors u and v are,

$$\begin{aligned} u_s(\mathbf{k}) &= \left[\sqrt{\frac{1+S}{2}} + \sqrt{\frac{1-S}{2}} \hat{k} \cdot \vec{\alpha} \right] u_s(0) \\ v_s(\mathbf{k}) &= \left[\sqrt{\frac{1+S}{2}} - \sqrt{\frac{1-S}{2}} \hat{k} \cdot \vec{\alpha} \right] v_s(0) \end{aligned} \quad (22)$$

Where $S = \sin(\varphi)$, $C = \cos(\varphi)$ and φ is a chiral angle which in the non condensed case is equal to $a \tan \frac{m}{k}$, but is not determined from the onset when chiral symmetry breaking occurs. In fact it will only be determined when the mass gap equation will be solved. This formalism is convenient to simplify the BS equation into the Salpeter equation, in a form which is as close as possible to the more intuitive Schrödinger equation. In order to have simple Weyl propagators from now on, we choose to redefine the vertices of the effective potential which now include the spinors u and v . The Dirac vertex γ_0 is now replaced by $u^\dagger u, u^\dagger v, v^\dagger u$ or $v^\dagger v$ when the vertex is respectively connected to a quark, a pair creation, a pair annihilation or an antiquark.

B. The BCS mass gap equation

The quark propagator is obtained when one calculates the self energy (2) and substitutes it self-consistently in the equation (10). Any solution of this equation \mathcal{S} must fulfill the MGE which insures that the vacuum is stable. One of the possible equivalent methods to insure the stability of the vacuum is to forbid the \mathcal{S}^{-1} , which plays the role of the effective quadratic term in the Lagrangian, to generate scalars directly from the vacuum. Otherwise the vacuum would be unstable. The mass gap equation is then,

$$\begin{aligned} 0 &= \dots \left\langle f_0 \right\rangle S^{-1} \\ &= \dots \left\langle f_0 \right\rangle \left[\mathcal{S}_0^{-1} - \text{loop diagrams} \right], \end{aligned} \quad (23)$$

where this is equivalent to state that the propagator must be diagonal. The quark (antiquark) one-body energy is obtained from the diagonal part of the propagator, and the cancellation of the anomalous (in the sense that it is not diagonal) part of the propagator produces the mass gap equation,

$$\begin{aligned} E(k) &= u_s^\dagger(k) \left\{ k \hat{k} \cdot \vec{\alpha} - \int \frac{dw'}{2\pi} \frac{d^3 k'}{(2\pi)^3} V(k-k') i \sum_{s'} \right. \\ &\quad \left. \left[\frac{u_{s'}(k') u_{s'}^\dagger(k')}{w' - E(k') + i\epsilon} - \frac{v_{s'}(k') v_{s'}^\dagger(k')}{-w' - E(k') + i\epsilon} \right] \right\} u_s(k), \\ 0 &= u_s^\dagger(k) \left\{ k \hat{k} \cdot \vec{\alpha} - \int \frac{dw'}{2\pi} \frac{d^3 k'}{(2\pi)^3} V(k-k') i \sum_{s'} \right. \\ &\quad \left. \left[\frac{u_{s'}(k') u_{s'}^\dagger(k')}{w' - E(k') + i\epsilon} - \frac{v_{s'}(k') v_{s'}^\dagger(k')}{-w' - E(k') + i\epsilon} \right] \right\} v_{s''}(k). \end{aligned} \quad (24)$$

where we used the limit of massless quarks. In the case of an instantaneous interaction, the loop integral in the energy w removes the pole in the propagator,

$$\int \frac{dw}{2\pi} \frac{i}{w - E(k) + i\epsilon} = \frac{1}{2} \quad (25)$$

and in the case of a quadratic interaction, the loop integral in the momentum is transformed in a Laplacian, see eq.(18). It is convenient to use [22,6] the quark energy projectors,

$$\begin{aligned} \sum_s u_s u_s^\dagger &= \Lambda^+ = \frac{1}{2} (1 + S\beta + C\hat{k} \cdot \vec{\alpha}), \\ \sum_s v_s v_s^\dagger &= \Lambda^- = \frac{1}{2} (1 - S\beta - C\hat{k} \cdot \vec{\alpha}), \end{aligned} \quad (26)$$

and other useful properties are,

$$\begin{aligned}
u_s^\dagger u_{s'} &= 1\delta_{ss'} \quad , \quad u_s^\dagger v_{s'} = 0\vec{\sigma} \cdot \vec{k}i\sigma_2 \\
u_s^\dagger \beta u_{s'} &= S\delta_{ss'} \quad , \quad u_s^\dagger \beta v_{s'} = -C\vec{\sigma} \cdot \vec{k}i\sigma_2 \\
u_s^\dagger \vec{\alpha} \cdot \vec{k} u_{s'} &= C\delta_{ss'} \quad , \quad u_s^\dagger \vec{\alpha} \cdot \vec{k} v_{s'} = S\vec{\sigma} \cdot \vec{k}i\sigma_2 \\
u_s^\dagger \beta \vec{\alpha} \cdot \vec{k} u_{s'} &= 0\delta_{ss'} \quad , \quad u_s^\dagger \beta \vec{\alpha} \cdot \vec{k} v_{s'} = 1\vec{\sigma} \cdot \vec{k}i\sigma_2 .
\end{aligned} \tag{27}$$

We get finally,

$$\begin{aligned}
E(k) &= kC + \frac{U}{2} + \frac{1}{2} [S\Delta(S) + C\hat{k} \cdot \Delta(\hat{k}C)] \\
&= \frac{U}{2} + kC - \frac{\varphi'^2}{2} - \frac{C^2}{k^2} ,
\end{aligned} \tag{28}$$

$$\begin{aligned}
0 &= \left\{ kS + \frac{1}{2} [-C\Delta(S) + S\hat{k} \cdot \Delta(\hat{k}C)] \right\} \vec{\sigma} \cdot \vec{k}i\sigma_2 \\
&= -(k^2\varphi')' + 2k^3S - 2SC .
\end{aligned} \tag{29}$$

C. from the BS S matrix to the Salpeter ladder and Schrödinger equations

When the interaction is instantaneous, a simplification occurs. For instance the BS amplitude has usually 4 independent components which are now expressed in terms of simply 2 wave functions ϕ^+ and ϕ^- ,

$$\begin{aligned}
\Rightarrow \text{Dirac} &= \left[\begin{array}{c} \text{diagram 1} + \text{diagram 2} \\ \text{diagram 3} + \text{diagram 4} \end{array} \right]_{Weyl} , \\
&= S_{q_1} u_1 u_1^\dagger(\chi) u_2 u_2^\dagger S_{q_2} + S_{q_1} u_1 (E - T_1 - T_2) \phi^+ v_2^\dagger S_{\bar{q}_2} + \\
&S_{\bar{q}_1} v_1 (-E - T_1 - T_2) \phi^{-t} u_2^\dagger S_{q_2} + S_{q_1} v_1 v_1^\dagger(\chi) v_2 v_2^\dagger S_{q_2} , \\
\chi &= -i \int \tilde{V} \left(u_1 \phi^+ v_2^\dagger + v_1 \phi^{-t} u_2^\dagger \right) = \triangleleft \chi \triangleright ,
\end{aligned} \tag{30}$$

where χ is proportional to the truncated BS amplitude and can also be represented graphically with a triangle. The S matrix in the ladder approximation has only 4 independent sub-matrices, that are calculated iteratively,

$$\begin{aligned}
\text{Diagram 1} &= \text{Diagram 2} + \text{Diagram 3} + \text{Diagram 4} \quad E \\
\text{Diagram 5} &= \text{Diagram 6} + \text{Diagram 7} \quad -E \\
\text{Diagram 8} &= \text{Diagram 9} + \text{Diagram 10} \quad E \\
\text{Diagram 11} &= \text{Diagram 12} + \text{Diagram 13} \quad -E
\end{aligned} \tag{31}$$

The other 12 sub-matrices are calculated from the independent 4 ones. The Salpeter equations are obtained when all the relative quark-antiquark energies of the system (31) are integrated,

$$\begin{aligned}
&\int \frac{dw}{2\pi} \frac{i}{w + E/2 - T_q + i\epsilon} \frac{i}{w + E/2 - T_{\bar{q}} + i\epsilon} = \\
&\frac{i}{E - T_q - T_{\bar{q}} + i\epsilon} ,
\end{aligned} \tag{32}$$

The Salpeter equations can then be written in the compact form,

$$\begin{aligned}
S &= G_0 + G_0 V S \\
\Rightarrow (G_0^{-1} - V) S &= 1 \\
\Rightarrow (E\sigma_3 - H + i\epsilon) S &= i
\end{aligned} \tag{33}$$

where σ_3 is the Pauli matrix,

$$\begin{aligned}
S &= \begin{bmatrix} S^{++} & S^{+-} \\ S^{-+} & S^{--} \end{bmatrix} , \\
G_0 &= \begin{bmatrix} \frac{i}{E - T_q - T_{\bar{q}} + i\epsilon} & 0 \\ 0 & \frac{i}{-E - T_q - T_{\bar{q}} + i\epsilon} \end{bmatrix} , \\
V &= -i \begin{bmatrix} \int V_d & \int V_a \\ \int V_a & \int V_d \end{bmatrix} , \\
H &= \begin{bmatrix} T_q + T_{\bar{q}} + \int V_d & \int V_a \\ \int V_a & T_q + T_{\bar{q}} + \int V_d \end{bmatrix}
\end{aligned} \tag{34}$$

and it turns out that H is an hermitian and positive operator.

The Salpeter wave-functions are the solutions of the homogeneous equations,

$$(E\sigma_3 - H)\phi = 0 , \quad \phi = \begin{pmatrix} \phi^+ \\ \phi^- \end{pmatrix} \tag{35}$$

which is an eigenvalue equation, similar to the Schrödinger equation, except for the σ_3 . This formalism is known as the energy-spin formalism. The Salpeter equation (35) is equivalent to the variational equation,

$$\delta \left(\frac{\langle \phi | H | \phi \rangle}{\langle \phi | \sigma_3 | \phi \rangle} \right) = 0 , \quad (36)$$

which suggests that a normalizing condition of the wave functions might be,

$$\langle \phi | \sigma_3 | \phi \rangle = |\phi^+|^2 - |\phi^-|^2 = 1 . \quad (37)$$

Let us study the class of solutions ϕ_u where this norm is possible, i. e. $|\phi_u^+| > |\phi_u^-|$. Once the single quark energies T and the 2-quark diagonal V_d and antidiagonal V_a potentials are defined, the solutions can be obtained numerically, either iteratively or variationally, and one finds a whole spectrum of solutions with energy $M > 0$. When M increases, we find that $|\phi_u^-|$ is proportional to M^{-1} , and in the limit of large mass we exactly recover Schrödinger equation. However another class of solutions ϕ_d is unavoidable, with a one to one correspondence with the ϕ_u , and where $|\phi_d^-| > |\phi_d^+|$,

$$\begin{aligned} \phi_d^+ &= \phi_u^- , \quad \phi_d^- = \phi_u^+ , \quad M_d = -M_u \\ \langle \phi_u | \sigma_3 | \phi_u \rangle &= 1 , \quad \langle \phi_d | \sigma_3 | \phi_d \rangle = -1 \end{aligned} \quad (38)$$

thus the spectrum is unbound. Exactly half of the solutions have a negative mass and a negative norm. When we include the infinitesimal $i\epsilon$ in eq. (35), we find that the larger component of ϕ dominates and the eigenvalues are now,

$$\begin{aligned} M_u &\rightarrow M_u - i\epsilon \\ M_d &\rightarrow M_d + i\epsilon = -(M_u - i\epsilon) \end{aligned} \quad (39)$$

The operators H and σ_3 are both hermitian, thus the set of solutions $|\phi\rangle$ constitute a basis of the Hilbert space, orthogonal in the sense that $\langle \phi | \sigma_3 | \phi' \rangle = 0$, and the identity element is,

$$1 = \sum \frac{\sigma_3 |\phi\rangle \langle \phi|}{\langle \phi | \sigma_3 | \phi \rangle} = \sum_u \sigma_3 |\phi\rangle \langle \phi| - \sum_d \sigma_3 |\phi\rangle \langle \phi| \quad (40)$$

Inserting this partition in the S matrix equation (33), we find,

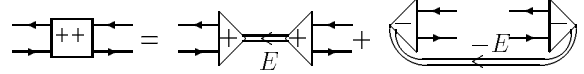
$$\begin{aligned} i &= (E\sigma_3 - H)S \\ &= \sum \frac{\sigma_3 |\phi\rangle \langle \phi|}{\langle \phi | \sigma_3 | \phi \rangle} (E\sigma_3 - H + i\epsilon) \sigma_3 \sum \frac{\sigma_3 |\phi\rangle \langle \phi|}{\langle \phi | \sigma_3 | \phi \rangle} \sigma_3 S \\ &= \sum \sigma_3 |\phi\rangle \frac{E - M + i\epsilon \langle \phi | \sigma_3 | \phi \rangle}{\langle \phi | \sigma_3 | \phi \rangle} \langle \phi | \sigma_3 S \\ \sigma_3 S &= \sum \sigma_3 |\phi\rangle \frac{i \langle \phi | \sigma_3 | \phi \rangle}{E - M + i\epsilon \langle \phi | \sigma_3 | \phi \rangle} \langle \phi | \\ S &= \sum_u |\phi_u\rangle \frac{i}{E - M_u + i\epsilon} \langle \phi_u | \\ &\quad - \sum_d |\phi_d\rangle \frac{i}{E - M_d - i\epsilon} \langle \phi_d | \end{aligned} \quad (41)$$

and the states with negative energy and negative norm can be reinterpreted as boundstates with positive mass

moving forward in time, where the variable $E = P_0$ in the propagator turns out to be negative,

$$\begin{aligned} S &= \sum_u |\phi_u\rangle \frac{i}{E - M_u + i\epsilon} \langle \phi_u | \\ &\quad + \sigma_1 |\phi_u\rangle \frac{i}{-E - M_u + i\epsilon} \langle \phi_u | \sigma_1 \end{aligned} \quad (42)$$

and it suffices to work with the ϕ_u . Diagrammatically we get for instance,

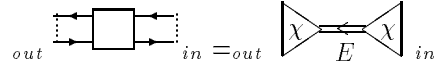


$$\text{Box}^{++} = \text{Box}^{++}_E + \text{Box}^{--}_{-E} \quad (43)$$

and it is consistent to substitute the $_d$ wave-functions and masses in terms of the components ϕ_u^+ , ϕ_u^- and the masses M_u . From now on this reinterpretation will be assumed and we will skip the subindex $_u$. The practical result is that we can use the amplitude ϕ^+ when the bra precedes the ket, and we use the amplitude ϕ^- for the opposite case. The closure of the identity now appears in the form,

$$\begin{aligned} 1 &= \sum |\phi^+\rangle \langle \phi^+| - |\phi^-\rangle \langle \phi^-| \\ 0 &= \sum |\phi^+\rangle \langle \phi^-| - |\phi^-\rangle \langle \phi^+| \end{aligned} \quad (44)$$

We now extend this reinterpretation to the truncated BS amplitudes χ and get for Dirac fermions,



$$\text{Box}^{out,in} = \text{Box}^{out,in}_E \quad (45)$$

D. The pseudoscalar and scalar solutions to the Salpeter equation

The homogeneous Salpeter equation for a meson is,

$$\begin{aligned} \frac{M - E_1 - E_2}{i} \phi^+ &= u_1^\dagger \chi v_2 \\ \frac{-M - E_1 - E_2}{i} \phi^{-t} &= v_1^\dagger \chi u_2 \\ \chi &= \int \frac{d^3 k}{(2\pi)^3} -iV(k) \left(u_1 \phi^+ v_2^\dagger + v_1 \phi^{-t} u_2^\dagger \right) \end{aligned} \quad (46)$$

where $k_1 = k + \frac{P}{2}$, $k_2 = k - \frac{P}{2}$, and this equation has to be solved numerically. The groundstate of the pseudoscalar channel constitutes an important solution of the Salpeter equation. This is the only case where the component ϕ^+ is comparable to the component ϕ^- , where the Schrödinger equation is not a good approximation to the Salpeter equation. We need to know this wave-function both for large and small center of mass momenta P of the bound state.

The small P limit of this model was already studied extensively in the literature [22]. For instance the Salpeter equation in the center of mass is,

$$\left\{ \left(-\frac{d^2}{dk^2} + 2E(k) \right) \begin{bmatrix} 1 & 0 \\ 0 & 1 \end{bmatrix} + \left(\frac{\varphi'^2}{2} + \frac{C^2}{k^2} \right) \begin{bmatrix} 1 & 1 \\ 1 & 1 \end{bmatrix} - M \begin{bmatrix} 1 & 0 \\ 0 & -1 \end{bmatrix} \right\} \begin{pmatrix} \phi^+ \\ \phi^- \end{pmatrix} = 0 \quad (47)$$

The *momentum* \otimes *spin* solution in the limit of small P is [22,11],

$$\begin{aligned} \phi^+ &= \mathcal{N}^{-1} \left(S + E_M f_1 + i g_1 \vec{P} \cdot \hat{k} \times \vec{\sigma} \right) \frac{i\sigma_2}{\sqrt{2}} \\ \phi^- &= \mathcal{N}^{-1} \left(-S + E_M f_1 - i g_1 \vec{P} \cdot \hat{k} \times \vec{\sigma} \right) \frac{i\sigma_2}{\sqrt{2}} \\ \mathcal{N}^2 &= 4E_M \int \frac{d^3k}{(2\pi)^3} S f_1 = (2f_\pi^{(t)})^2 E_M \\ E_M &= \sqrt{\frac{f_\pi^{(s)}}{f_\pi^{(t)}}} P, \quad f_\pi^{(t)} = .08, \quad f_\pi^{(s)} = .77 \end{aligned} \quad (48)$$

see [22,11] for $f_\pi^{(t)}$, $f_\pi^{(s)}$ and for the functions f_1 , g_1 which turn out to be quite small.

We now discuss the other limit of large momentum P , where the chiral angle φ , depicted in Fig. [6] vanishes faster than exponentially. The vertices, up to first order in P^{-1} are,

$$\begin{aligned} u_s^\dagger(k + \frac{P}{2}) u_{s'}(k' + \frac{P}{2}) &\simeq \delta_{ss'} - i\vec{\sigma}_{ss'} \cdot \hat{P} \times (\vec{k} - \vec{k}') \frac{1}{P} \\ v_s^\dagger(k + \frac{P}{2}) v_{s'}(k' + \frac{P}{2}) &\simeq \delta_{ss'} - (i\vec{\sigma}_{ss'}^*) \cdot \hat{P} \times (\vec{k} - \vec{k}') \frac{1}{P} \\ u_s^\dagger(k + \frac{P}{2}) v_{s'}(k' + \frac{P}{2}) &\simeq (\vec{k}_\perp - \vec{k}'_\perp) (\sigma i\sigma_2)_{ss'} \frac{1}{P} \\ v_s^\dagger(k + \frac{P}{2}) u_{s'}(k' + \frac{P}{2}) &\simeq -(\vec{k}_\perp - \vec{k}'_\perp) (\sigma i\sigma_2)_{ss'}^* \frac{1}{P} \end{aligned} \quad (49)$$

where the index \perp denotes the projection $\vec{k} - (\vec{k} \cdot \hat{P})\hat{P}$ of a vector \vec{k} in the plane perpendicular to \vec{P} . Up to first order in P the equation for a positive energy boundstate function $\phi^+(k) i\sigma_2 / \sqrt{2}$ is,

$$\left(P + \frac{2k^2}{P} - M - \Delta_k \right) \phi^+ - 2i \frac{\hat{P}}{P} \times \vec{\nabla} \cdot \{ \vec{\sigma}, \phi^+ \} \simeq 0 \quad (50)$$

The most general pseudoscalar wave function is of the form,

$$\phi^+(k) = \phi_0(k) + i\vec{\sigma} \cdot \hat{P} \times \vec{k} \phi_1(k) \quad (51)$$

and it turns out, after solving the equation (50), that the ϕ_1 component is vanishing and that only the simple ϕ_0 component remains. We now estimate in this limit

the negative energy component of the pseudoscalar meson. We find for the Salpeter equation with the harmonic confining potential, a 1S_0 solution with equation,

$$\begin{bmatrix} P + 2\frac{k^2}{P} - \Delta_k - M & \frac{-4}{P^2} \\ \frac{-4}{P^2} & P + 2\frac{k^2}{P} - \Delta_k + M \end{bmatrix} \begin{pmatrix} \phi^+ \\ \phi^- \end{pmatrix} \simeq 0 \quad (52)$$

The *momentum* \otimes *spin* solution up to highest order in P , is a Gauss function,

$$\begin{aligned} \phi^+ &= \phi_p(k) \frac{i\sigma_2}{\sqrt{2}}, \quad \phi^- \simeq \frac{-2}{P^3} \phi^+ \\ \phi_p(k) &= \frac{e^{\frac{-k^2}{2\alpha_p^2}}}{N_p}, \quad N_p^{-1} = \left(\frac{2\sqrt{\pi}}{\alpha_p} \right)^{3/2}, \quad \alpha_p^2 = \sqrt{\frac{P}{2}} \end{aligned} \quad (53)$$

For large momentum P we find that ϕ^+ is quite flat in k , while ϕ^- is almost negligible. This result is consistent with the relativistic space contraction.

The Salpeter equation for the scalar in the center of mass is,

$$\left\{ \left(-\frac{d^2}{dk^2} + 2E(k) - \frac{2}{k^2} \right) \begin{bmatrix} 1 & 0 \\ 0 & 1 \end{bmatrix} + \left(\frac{\varphi'^2}{2} - \frac{C^2}{k^2} \right) \begin{bmatrix} 1 & 1 \\ 1 & 1 \end{bmatrix} - M \begin{bmatrix} 1 & 0 \\ 0 & -1 \end{bmatrix} \right\} \begin{pmatrix} \phi^+ \\ \phi^- \end{pmatrix} = 0 \quad (54)$$

It turns out that the negative energy ϕ^- component for the groundstate is less than 10% of the positive energy component ϕ^+ . The Schrödinger limit, where only the positive energy component is considered, is therefore acceptable. The *momentum* \otimes *spin* solution for the scalar is very close to a Gaussian,

$$\begin{aligned} \phi^+ &\simeq \phi_s(k) \vec{K} \cdot \vec{\sigma} \frac{i\sigma_2}{\sqrt{2}}, \quad \phi^- \simeq 0.1 \phi^+ \\ \phi_s(k) &= \frac{e^{\frac{-k^2}{2\alpha_s^2}}}{N_s}, \quad N_s^{-1} = \frac{4\sqrt{\pi\sqrt{\pi}}}{\sqrt{3}\alpha_s^{5/2}}, \quad \alpha_s \simeq .857 \end{aligned} \quad (55)$$

E. Infrared finite coupled channels in the BCS approximation

The step from the ladder approximation to a boundstate equation with coupled channels is not perturbative in the parameters of the microscopic model. This is not achieved with a series expansion in the potential strength K_0 or the number of colors N_c . The relevant degrees of freedom of low energy hadronic phenomenology are the bosonic mesons and fermionic hadrons. At the bare level they correspond respectively to $q\bar{q}$ and qqq ladders. To achieve this hadronization we consider the complete series of diagrams that contribute to the irreducible $q\bar{q}$ interaction. One has to include all the possible number of

quark loops and the possible insertion of the microscopic quark-quark interaction. Then this series can be resumed in order to factorize the bare meson and hadron ladders. The microscopic interactions that remain isolated are responsible for the interactions and couplings of the bare hadrons. In order to simplify the calculations it is convenient to truncate eventually the series of diagrams. The perturbative parameter is then the number of considered ladders. This is both straightforward and also close to the hadronic phenomenology. As we mentioned, this step may remain consistent with the BCS level, if its feedback in the mass gap equation is negligible.

In the case of an instantaneous microscopic interaction, the hadronic equations are analogous to the Resonating Group Method. The ladder itself has less independent amplitudes than in the case of time-dependent interactions. The complete set of bare mesons is described by the integral $\int \frac{dw}{2\pi}$ of the ladder in the relative energies of the quark-antiquark ladder. The integral is necessary to originate a single pole in G_0 . To ensure in a particular diagram that the meson poles are present it is convenient to decompose the ladder in,

$$\text{Ladder} = \text{Bare Ladder} + \text{Ladder with Quark Loop} + \text{Ladder with Quark Loop and Meson Pole} \quad (56)$$

where the first pair of diagrams may for instance contribute to the overlap interaction between a pair of mesons and may not include a ladder.

At the BCS level the infinite infrared divergent constant U is extremely convenient [26] to remove the colored states, which have masses proportional to U ,

$$\sum_i T_i + \sum_{i < j} V_{ij} \simeq \frac{U}{2} \left| \sum_i \frac{\lambda_i}{2} \right|^2. \quad (57)$$

In this model of confinement, the masses of color singlets are independent of U . We now show that the interactions of color singlets are equally finite. The hadron-hadron interactions are built from the quark-quark microscopic interaction (18) in two different processes. When the number of hadrons are conserved, this is for instance the case in elastic scattering, we have quark exchange overlaps,

$$\text{Quark Exchange Overlap} = \text{Bare Overlap} + \text{Overlap with Quark Loop} + \text{Overlap with Quark Loop and Meson Pole} \quad (58)$$

and when a hadron is emitted or absorbed we have quark-antiquark annihilation overlaps, for instance,

$$\text{Quark-Antiquark Annihilation Overlap} = \text{Bare Annihilation Overlap} + \text{Annihilation Overlap with Quark Loop} \quad (59)$$

We now show that the effect is finite, starting by the integration of the relative energies in the first diagrams of respectively eq. (58) and eq(59),

$$\begin{aligned} & \int \frac{dw}{2\pi} \frac{i}{w - T_1 + i\epsilon} \frac{i}{-w - T_4 + i\epsilon} \frac{i}{w - T_3 + i\epsilon} \frac{i}{-w - T_2 + i\epsilon} \\ &= i(T_1 + T_2 + T_3 + T_4) G_{0a} G_{0b} G_{0c} G_{0d} \\ & \int \frac{dw dw'}{(2\pi)^2} \frac{i}{w - T_1 + i\epsilon} (-iV_{13}) \frac{i}{w' - T'_1 + i\epsilon} \frac{i}{-w' - T'_4 + i\epsilon} \\ & \frac{i}{w' - T'_3 + i\epsilon} \frac{i}{w - T_3 + i\epsilon} \frac{i}{-w - T_2 + i\epsilon} \\ &= -iV_{13} G_{0a} G_{0b} G_{0c} G_{0d}, \\ & \int \frac{dw dw'}{(2\pi)^2} \frac{i}{w - T_1 + i\epsilon} iV_{1\bar{4},3} \frac{i}{-w' - T'_4 + i\epsilon} \\ &= \frac{i}{w' - T'_3 + i\epsilon} \frac{i}{w - T_3 + i\epsilon} \frac{i}{-w - T_2 + i\epsilon} \\ &= -iV_{1\bar{4},3} G_{0a} G_{0b} G_{0c}. \end{aligned} \quad (60)$$

where the G_{0n} are in fact part of the respective BS amplitudes which are untruncated. In the case of the exchange overlap, the remaining factors are,

$$\begin{aligned} & i(T_1 + T_2 + T_3 + T_4 - V_{13} - V_{24}) P_{13} \\ &= i(T_1 + T_2 + T_3 + T_4 + V_{14} + V_{23}) P_{13} \\ &= iP_{13}(T_1 + T_2 + V_{12} + T_3 + T_4 + V_{34}) \\ &= iP_{13}(0U + \dots) \end{aligned} \quad (61)$$

where the infinite $-U$ terms cancel because the mesons 32 and 14 in the left and 12 and 34 in the right are color singlets. The remaining result . In the case of the annihilation overlap, the remaining factor is $-iV_{1\bar{4},3}$. It is also finite because the quark-antiquark annihilation vertex is independent of U since $v_s^\dagger(k) \delta^3(k - k') u_{s'}(k') = 0$. We find that all the terms proportional to U cancel when the complete set of diagrams which contribute to the interaction between color singlets is included.

We conclude that in this framework the model is finite. First the masses of bare hadrons and their interactions are evaluated. Then we compute the masses and widths of dressed hadrons. These are the final freedom degrees which can be compared with the experimental spectrum of hadronic resonances.

F. The coupling of a scalar to a pair of pseudoscalars

The form factor for the coupling of a scalar f_0 to a pair of π can be expressed either with Salpeter wave-functions or Bethe-Salpeter amplitudes,

$$\text{Triangle Diagram} = \text{Triangle Diagram with } S^{-1} \text{ and (B. S.)} \quad (B. S.) =$$

$$+ \quad + \quad + \quad (S.) \quad (62)$$

The form factor can be decomposed in diagrams where a quark (antiquark) line either emits (absorbs) a pseudoscalar or a scalar. While in the Dirac formalism the coupling of a meson to a quark line is just the truncated Bethe-Salpeter amplitude χ , in the equivalent Goldstone-Weyl formalism the coupling of a meson to a quark line is $u^\dagger \chi u$.

We first consider the limit of a coupling to pions of low momentum P . The coupling of the pseudoscalar to the quark is derivative and thus is suppressed. For instance in the case of a massless π in the center of mass,

$$\begin{aligned} \phi^+(k, 0) &= \mathcal{N}^{-1} S \frac{i\sigma_2}{\sqrt{2}}, \quad \phi^-(k, 0) = -\phi^+(k, 0) \\ u\phi^+ v^\dagger + v\phi^- u^\dagger &= \sqrt{2} \mathcal{N}^{-1} S \beta \gamma_5 \\ u^\dagger(k) \chi(k, 0) u(k) &= -u^\dagger(k) \Delta \left(\frac{\sqrt{2} S \beta \gamma_5}{\mathcal{N}} \right) u(k) = 0. \end{aligned} \quad (63)$$

The dominant contribution includes the coupling of the 3P_0 scalar meson to the quark (antiquark) line. Due to the large mass of the scalar meson, the negative energy wave-function is negligible. The positive energy *momentum* \otimes *spin* wave-function, in the center of mass frame, is shown in eq. (55). The truncated BS amplitude is,

$$\begin{aligned} \chi_s &= -\Delta u_{s_1} k \phi_s(k) \frac{[\vec{\sigma} \cdot \hat{k} i \sigma_2]_{s_1 s_2} u_{s_2}^\dagger}{\sqrt{2}} \\ &= -\Delta \frac{2k \phi_s(k)}{1+S} \Lambda^+ u_{s_1}(0) \frac{[\vec{\sigma} \cdot \hat{k} i \sigma_2]_{s_1 s_2}}{\sqrt{2}} u_{s_2}^\dagger(0) i \alpha_2 \gamma_5 \Lambda^- \\ &= -\Delta \frac{-2k \phi_s(k)}{1+S} \Lambda^+ \frac{1+\beta}{2} \frac{\vec{\alpha} \cdot \hat{k}}{\sqrt{2}} \Lambda^- \\ &= \Delta \frac{\Lambda^+ \beta \vec{\alpha} \cdot \vec{k} \phi_s(k)}{\sqrt{2}} \end{aligned} \quad (64)$$

The scalar coupling $u^\dagger(k) \chi_s(k) u(k)$ to the quark line is,

$$\begin{aligned} u_{s_1}^\dagger \chi_s(k) u_{s_2} &= \frac{\delta s_1 s_2}{2\sqrt{2}} \left[C \hat{k} \cdot \Delta(\hat{k} S k \phi) - S \Delta(C k \phi) \right] \\ &= \frac{\delta s_1 s_2}{\sqrt{2}} \left[\left(-\frac{CS}{k^2} + \frac{\varphi''}{2} + \frac{\varphi'}{k} \right) k \phi_s + (k \phi_s)' \varphi' \right] \\ &= \frac{\delta s_1 s_2}{\sqrt{2}} \left[\left(-\frac{2CS}{k^2} + kS \right) k \phi_s + (k \phi_s)' \varphi' \right] \end{aligned} \quad (65)$$

except for the $-i$ factor which goes with any potential insertion according to the Feynman rules. We will discard it in this section. The coupling $f(P)$ to a pair of pions with low momentum P is,

$$\begin{aligned} f &= \text{tr} \int \frac{d^3 k}{(2\pi)^3} \left(\frac{-S i \sigma_2}{\mathcal{N} \sqrt{2}} \right)^\dagger \left(u^\dagger \chi_s u \frac{S i \sigma_2}{\mathcal{N} \sqrt{2}} + \frac{S i \sigma_2}{\mathcal{N} \sqrt{2}} v^\dagger \chi_s v \right) \\ &= \int \frac{d^3 k}{(2\pi)^3} \frac{S^2}{\sqrt{2} \mathcal{N}^2} \left[\left(-\frac{2CS}{k^2} + kS \right) k \phi_s + (k \phi_s)' \varphi' \right] \\ &= \frac{-0.47}{P}. \end{aligned} \quad (66)$$

We find that the coupling $f(P)$ is proportional to f_π^{-2} which in this model is quite large. We thus find a large coupling of a scalar to a pseudoscalar pair in the small P limit.

We now consider the opposite limit of large pion momentum P . In this case the negative energy component of the pion is quite small. We expect that the dominant diagrams include the positive energy ϕ^+ which is shown in eq. (53), which is present in either the coupling of a pion to the quark line,

$$\begin{aligned} &\int \frac{d^3 k'}{(2\pi)^3} V(k-k') u^\dagger(k+P/2) v(k'+P/2) \\ &\quad \phi_p(k', P) \frac{i\sigma_2}{\sqrt{2}} v^\dagger(k'-P/2) u(k-P/2) \\ &\simeq \sqrt{2} \left(\vec{\nabla}_k \phi_p(k, P) + i\vec{\sigma} \times \frac{\hat{P}}{P} \phi_p(k, P) \right) \cdot \frac{1}{P} \vec{\sigma}_\perp \\ &= \frac{\sqrt{2}}{P} \left[\vec{\nabla}_k \phi_p \cdot \vec{\sigma}_\perp + \frac{2}{P} \phi_p \hat{P} \cdot \vec{\sigma} \right] \end{aligned} \quad (67)$$

or the coupling of a π to an antiquark line,

$$-\frac{\sqrt{2}}{P} \left[\vec{\nabla}_k \phi_p \cdot \vec{\sigma}_\perp^* + \frac{2}{P} \phi_p \hat{P} \cdot \vec{\sigma}^* \right] \quad (68)$$

where eqs. (49) were used to produce the result at the highest order in P . The total coupling is a functional of the scalar and pseudoscalar wavefunctions, which are described in eqs. (53,55) by Gaussians. We find for the *momentum* \otimes *spin* coupling,

$$\begin{aligned} f(P) &= \text{tr} \int \frac{d^3 k}{(2\pi)^3} \left[\phi_s(k+P/2) (\vec{k} + \vec{P}/2) \cdot \vec{\sigma} \frac{i\sigma_2}{\sqrt{2}} \right]^\dagger \\ &\quad \left[\frac{\sqrt{2}}{P} \left(\vec{\sigma}_\perp \cdot \vec{\nabla} \phi_p(k) + \frac{2}{P} \vec{\sigma} \cdot \hat{P} \phi_p(k) \right) \phi_p(k) \frac{i\sigma_2}{\sqrt{2}} \right. \\ &\quad \left. - \phi_p(k) \frac{i\sigma_2}{\sqrt{2}} \frac{\sqrt{2}}{P} \left(\vec{\sigma}_\perp^* \cdot \vec{\nabla} \phi_p(k) + \frac{2}{P} \vec{\sigma}^* \cdot \hat{P} \phi_p(k) \right) \right] \\ &= \frac{2\sqrt{2}}{P} \int \frac{d^3 k}{(2\pi)^3} \phi_s \left(\vec{k} + \frac{\vec{P}}{2} \right) \cdot \left(\frac{2}{P} \hat{P} - \frac{1}{\alpha_p^2} \vec{k}_\perp \right) \phi_p^2 \\ &= \frac{43.6}{P/2} (1-1) \frac{\alpha_s^{5/2}}{\alpha_T^5} e^{-\frac{(P/2)^2}{\alpha_T^2}}, \quad \alpha_T^2 = 2\alpha_s^2 + \alpha_p^2 \end{aligned} \quad (69)$$

We find that the coupling cancels for the groundstate scalar in the highest order terms in P . The cancellation is specific to the scalar meson. Each of the canceling parts

is of the order of $2K_0^{-1/2}$ for P of the order of $2K_0$. The same technique can be used to compute the contribution from the nondominant terms which are quadratic on the negative energy component of the pion. In this case the ∇ is applied in both π wavefunctions instead of just one, and there is an extra factor of $-2/P^3$ due to the negative energy wavefunction. The coupling $f(P)$ is now,

$$f(P) = -\frac{10.9}{(P/2)^4} (1-2) \frac{\alpha_s^{5/2}}{\alpha_T^5} e^{-\frac{(P/2)^2}{\alpha_T^2}} \quad (70)$$

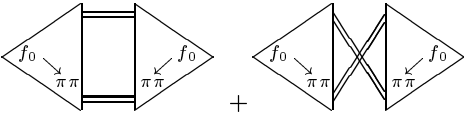
which is finite and is smaller than each of the canceling parts in eq. (69) by a factor of 4 in the case of a P of the order of $2K_0$. In this case $f(P)$ is of the order of $0.5 K_0^{-1/2}$.

The color factor for f_0 and π color singlets is $1/\sqrt{3}$. The flavor factor for the coupling of a scalar isosinglet $\frac{u\bar{u}+d\bar{d}}{\sqrt{2}}$ to a pair of pseudoscalar isovectors, say $u\bar{d}$ and $-d\bar{u}$, with a flavor independent quark-antiquark annihilation is $-1/\sqrt{2}$. The total coupling is then $-f(P)/\sqrt{6}$.

The result for a general momentum is very cumbersome to derive. For momenta of the order of K_0 , we will use the approximation of matching both limits with an interpolating function.

G. The $f_0(980) \rightarrow \pi\pi$ decay

The decay width of a f_0 in a pair of π can be calculated from the the Breit-Wigner pole in the meson propagator. We call bare the ladder meson, see eq. (4). The bare mass M_0 is real and is a solution of the Bethe-Salpeter equation. When coupled channels of mesons are included, the bare meson is dressed. The dressed pole is composed by the bare mass M_0 plus the coupled channel contribution which includes a real mass shift, and an imaginary term in the case where the mass is above the coupled thresholds. The mass is then,

$$M = M_0 + \Delta M, \quad \Delta M = -i\Sigma$$


$$\Sigma_{f_0} = \quad (71)$$

where we only included a loop of bare π , which is the simplest contribution to the scalar self energy. The integral in the loop energy provides an extra $2\pi i$ factor, which verifies that in general ΔM includes a real component, and we find that,

$$\Delta M = 6 \int \frac{d^3q}{(2\pi)^3} \frac{\frac{f(q)^*}{\sqrt{6}} \frac{f(q)}{\sqrt{6}}}{M_{f_0} - 2\sqrt{q^2 + M_\pi^2} + i\epsilon} \quad (72)$$

where the factor of 6 includes the 3 different flavors of the isovector π , and the factor 2 from the direct and exchange

diagram of the self energy in eq. (71). We are particularly interested in computing the width of the scalar f_0 which is measured experimentally. In this section we represents as usually the width of a resonance by a Γ , which should not to be confused with the same symbol which is used in other sections for the vector or axial vertices. The width Γ is a simple function of the imaginary component of ΔM ,

$$Im(\Delta M) = -i\frac{\Gamma}{2},$$

$$\Gamma = \frac{1}{4\pi} P M_{f_0} |f(P)|^2, \quad P = \frac{1}{2} \sqrt{M_{f_0}^2 - 4M_\pi^2}. \quad (73)$$

Let us consider the case of a scalar mass M_{f_0} of the order of $1 GeV$, where P is larger than the scale of the interaction by a factor of 2. In this case, it is sensible to use the limit of large P . We find in eq. (69) that the coupling $f(P)$ cancels for the scalar in the highest order terms in P . We first evaluate the width which we would obtain if this cancellation had not occurred. Each of the canceling contributions singled out, would yield a width Γ of $672 MeV$. Using the $f(P)$ of eq.(70), we find a width of just $42 MeV$ which lies within the experimental limits. However the theoretical error bars are quite large because the higher order terms of eq. (69) have not been computed yet.

The cancellation of eq. (69) is specific to the ground state $q\bar{q}$ scalar meson decaying into very light pseudoscalars. For instance the vector meson coupling has no cancellations. An excited scalar has no cancellations either and thus would show larger widths. In the case of a decay into heavier pseudoscalars such as the K , the cancellation does not hold since P is small. This is compatible with the observed widths of the $f_0(980)$ and $a_0(980)$ which is exceptionally narrow when compared with the widths of the other hadronic resonances.

III. GOING BEYOND BCS WITH FINITE COUPLED CHANNEL EFFECTS

A. The Equations for the Self Energy and the Vertex

We now go beyond BCS including the mesonic coupled channels (bBCSsc) both in the MGE and in the bound state equations. It is convenient to return to the Dirac formalism in order to reduce the number of diagrams when we apply the WI. We will extend the MGE for the self energy of the quarks with the simple one meson exchange. The naive extension would be to add to the self energy Σ of eq. (2) a new rainbow diagram where the effective quark-quark interaction is replaced by a ladder which is equivalent to a series of One Meson Exchange Potentials,

$$\Sigma_s(\vec{k}, w) = \text{Diagram (74)} \quad (74)$$

However this would lead to an incomplete set of diagrams in the corresponding Bound State Equation for dressed mesons. The coupled pair of mesons would interact directly through some diagrams which would not be the complete possible set. Σ_s also carries the technical difficulty of being a nonconstant function of the energy w , unlike the BCS self energy. Moreover Σ_s includes terms of order U which are infrared divergent. The effect of a new infrared divergent in the self energy was already studied [10]. The result is that the bare mesons which are derived from the ladder have a divergent mass, and thus are completely different from the dressed mesons which mass is finite. Then the perturbative expansion in the number of ladders is no longer acceptable. In order to circumvent all these troubles we prefer to restrict the self energy in a way that the pair of mesons do not interact directly. They are only allowed to interact indirectly through the annihilation into a single meson. In a similar fashion to the ladder of eq. (56), we have to include a pair of extra interactions in the self energy.

We find that the minimal extension of the mass gap equation beyond BCS is achieved with a new tadpole term in the self energy,

$$\Sigma = \text{[dashed line with arrow]} + \text{[loop diagram with } \Sigma_s \text{ label]} \quad (75)$$

which might seem more complex than Σ_s but in fact is a truncation because upon iteration Σ_s would generate this diagram and other ones too. It also turns out that the self energy of eq. (75) is now energy independent and does not carry a new infrared divergence. Using the WI prescription of inserting the vertex in all possible propagators, we arrive at the corresponding bound state equation for the vertex,

Figure 1 illustrates the reduction of a four-point function to a sum of two-point functions. The diagrams are arranged in five rows, each showing a four-point function (left) equal to a sum of two-point functions (right). The diagrams are labeled with various symbols, including Γ_0 , Σ_s , and Γ_s .

where the diagrams are shown in separate lines according to their properties. Line 1 corresponds to the BS equation at the BCS level. Without the other lines it would reproduce the ladder Bethe-Salpeter equation for the vertex. The lines 2, 3 and 5 were separated because they contain all the contain terms proportional to the infrared divergent U , but they cancel in each line and all lines are finite. The remaining lines 4 and 6 contain the terms that one would expect in coupled channel equations where a pair of mesons is created and then annihilated (except for the first diagram of line 4 which vanishes). With them we calculate for instance the partial decay width of a resonance into a channel of 2 mesons. The last lines 5 and 6 are only relevant for flavor singlets because the quark pair in the incoming meson is annihilated, thus for flavor vectors they are null. We now return to the Goldstone-Weyl formalism and show in more detail the properties of the diagrams in eq. (76).

The cancellation of the infrared divergences become clear in the Goldstone-Weyl formalism. Let us consider for instance the diagrams of line 2 in eq. (76),

(77)

These 3 diagrams are infrared divergent but their sum is finite, in an analogous way to eq. (58). It is important to remark that in the previous calculations in the literature, the extrapolation from the ladder level to the

coupled channel level would only include the diagrams of lines 4 and 6. We now find the previous choice arbitrary since the diagrams of lines 2, 3 and 5 were not considered. The role of these diagrams is to cancel any real mass shift of the π due to the usual coupled channel diagrams of lines 4 and 6, in order that the π remains a Goldstone boson in the chiral limit. This is ensured by the WI, see eq. (11). In this case we find no overall mass shift in the meson spectrum due to coupled channels. Only splittings between different levels may be affected by coupled channels.

It is convenient to have a box $\int VG_0V$ at the left of the remaining bBCSs diagrams in eq (76). Upon iteration the equation,

$$\Gamma = \Gamma_0 + V G_0 \Gamma + V G_0 V M \Gamma \quad (78)$$

can be resummed. If we factorize the S matrix at the ladder level $S_0 = (1 - G_0V)^{-1}G_0$, see eq. (33), the ladder will appear in the middle of the coupled channel terms,

$$\begin{aligned} G_0 \Gamma &= S_0 \Gamma_0 + S_0 V G_0 V M \Gamma \\ &= S_0 \Gamma_0 + G_0 V S_0 V M \Gamma, \\ \Gamma &= V (G_0 V)^{-1} S_0 \Gamma_0 + V S_0 V M \Gamma \\ &= V \frac{1}{1 - S_0 V M V} (G_0 V)^{-1} S_0 \Gamma_0 \\ &\simeq V \frac{i}{E - M_b - i V M V} \Gamma_0, \end{aligned} \quad (79)$$

where $V M V$ includes the irreducible factorization of the coupled channels with 2 mesons. In the pole of Γ , which is equivalent to the meson wave-function, we recover the Resonating Group Method equations for coupled channels of one meson and of a pair of non-interacting mesons. It can be checked that with a simpler self energy in eq.(75), for instance with Σ_s or without the box, terms which could be interpreted as an incomplete contributing to the direct interaction between the pair mesons of the coupled channel would appear. In this paper we follow the approximation of neglecting the four legged direct interaction of the pair of mesons.

We now study the terms which contribute to the widths of the resonances that could not be calculated at the BCS level. The imaginary component of the mass comes from the diagrams with at least two ladders. Only the second diagram of line 4 and the diagram of line 6 will contribute with

$$\int \frac{d^3 P dW}{(2\pi)^4} f^*(P) \frac{i}{W - E_{m1}(P) - E_{m2}(P) + i\epsilon} f(P) \quad (80)$$

Where E_{m1}, E_{m2} are the energies of the coupled mesons, and W, P is the 4-momentum which flows in the meson loop. The form factor for the coupling of the initial meson to the pair of mesons in the coupled channel is the function $f(P)$ which was computed in the previous section. In the same way the imaginary part of eq. (80) is

precisely $-i\Gamma/2$. Thus we recover the same formula that was used in previous calculations for the widths of resonances. The question now is how sensitive is the mass gap equation to the coupling of mesonic channels. Eventually we would like to know the feedback on the coupling $f(P)$ which is a functional of the chiral angle $\varphi(k)$.

B. The Mass Gap Equation

Using the Weyl fermions, and expanding the ladder in meson poles, we find that the self energy of the quark has a diagonal component Σ_d which contributes to the dynamical mass of the quark,

$$\Sigma_d = \text{---} \text{---} \text{---} + \text{---} \text{---} \text{---}, \quad (81)$$

and the self energy of the antiquark is exactly the same. We find that the energy of 1 quark is identical to the BCS one of eq. (28) except for the expected changes of the chiral angle φ . In eq.(81) we only included the nonvanishing diagrams which remain from an expansion in powers of $1/U$. The free Green functions are proportional to U^{-1} . The interactions without a pair creation or annihilation are proportional to the infinite infrared constant U , while the remaining interactions are finite. It turns out that the new coupled channel diagrams vanish. This happens because in the limit of an infinite $-U$ the box diagram in eq. (75) which contributes to the quark energy vanishes,

$$\begin{aligned} \text{---} \text{---} \text{---} &= 0, \quad \text{---} \text{---} \text{---} = 0, \quad \text{---} \text{---} \text{---} = \text{---} \text{---} \text{---}, \\ (a) \quad (b) \quad (c) \end{aligned} \quad (82)$$

however the corresponding diagram which contributes to the mass gap equation is finite.

The mass gap equation is obtained when we impose that the antidiagonal components Σ_a of the self must cancel. This postulate ensures vacuum stability. Otherwise these components would either create or annihilate quark-antiquark pairs in the vacuum. The diagrams that contribute to the antidiagonal component of the self energy in the mass gap equation are now,

$$\begin{aligned} \Sigma_a &= \text{---} \text{---} \text{---} + \text{---} \text{---} \text{---} + \text{---} \text{---} \text{---} + \text{---} \text{---} \text{---} \\ &+ \text{---} \text{---} \text{---} + \text{---} \text{---} \text{---} \end{aligned} \quad (83)$$

where we only show the energy dependence of the diagrams and where the lines --- only mean the presence of spinors u, v, u^\dagger or v^\dagger and don't include the quark

or anti-quark Goldstone-Weyl propagator. In eq.(83) we only show the diagrams which are nonvanishing in orders of $1/U$, and in fact they all turn out to be finite, of order U^0 . The first pair of diagrams are BCS diagrams. We will now concentrate on the new diagrams which depend on the Coupled Channels. We will for instance consider the third diagram of eq. (83). The integration of the quark propagators as a function of the relative energies yields,

$$\int \frac{dw}{2\pi} \frac{i}{w - T_1 + i\epsilon} \frac{i}{E - w - T_2 + i\epsilon} \frac{i}{w - T_{1'} + i\epsilon} = \frac{i}{E - T_1 - T_2 + i\epsilon} \frac{i}{E - T_{1'} - T_2 + i\epsilon}, \quad (84)$$

and we obtain a product of quark-antiquark G_0 . We now integrate the meson propagator,

$$\int \frac{dE}{2\pi} \frac{i}{-E - M_b + i\epsilon} \frac{i}{E - T_1 - T_2 + i\epsilon} \frac{i}{E - T_{1'} - T_2 + i\epsilon} = \frac{i}{-M_b - T_1 - T_2 + i\epsilon} \frac{i}{-M_b - T_{1'} - T_2 + i\epsilon}. \quad (85)$$

According to eq. (46), each of this denominators, together with the spinors v^\dagger and u will transform the χ Salpeter amplitude into a negative energy wave function ϕ^- . The result after integrating in all the loop energies is,

$$\Sigma_d(k) = \frac{1}{2} k \frac{s_1 s_2}{s_1 s_2} \frac{k'}{s_2 s_5} k + \frac{1}{2} k \frac{s_2 s_5}{s_2 s_5} \frac{k'}{s_1 s_2} k$$

$$\Sigma_a = \frac{1}{2} k \frac{s_1 s_2}{s_1 s_2} \frac{k'}{s_2 s_5} k + \frac{1}{2} k \frac{s_2 s_5}{s_2 s_5} \frac{k'}{s_1 s_2} k$$

$$+ \text{[Four meson exchange diagrams]} \quad (86)$$

All the mesons, except the π , have a negligible component ϕ^- , and this shows that the effect of the infinite tower of coupled channels is finite. We will now retain just the contribution of the π ladder. In this way the diagrams

which are present in the mass gap equation are similar to the ones of eq. (62); except for the scalar wavefunction, which folds from the left the coupling of the scalar to a pair of pseudoscalars, but is not included here.

We find that the quark energy $E = E_0 - \Sigma_d$ remains the BCS one of eqs. (24) to (28),

$$E(k) = u^\dagger(k) \vec{\alpha} \cdot \vec{k} u(k) - \frac{1}{2} \left\{ u^\dagger(k) \int \frac{d^3 k'}{(2\pi)^3} V(k - k') \left[\Lambda^+(k') - \Lambda^-(k') \right] u(k) \right\} \quad (87)$$

and the mass gap equation $0 = S_0^{-1} - \Sigma_a$ is now,

$$\begin{aligned} 0 = & +u_{s_1}^\dagger(k) \vec{\alpha} \cdot \vec{k} v_{s_5}(k) \\ & - \left\{ u_{s_1}^\dagger(k) \int \frac{d^3 k'}{(2\pi)^3} V(k - k') \left[\right. \right. \\ & + u_{s_2}(k') \left(\frac{\delta_{s_2 s_4}}{2} - \int \frac{d^3 P}{(2\pi)^3} \phi_{s_2 s_3}^-(P, k' - P/2) \right. \\ & \left. \left. \phi_{s_3 s_4}^-(P, k' - P/2) \right) u_{s_4}^\dagger(k') \right. \\ & \left. - v_{s_2}(k') \left(\frac{\delta_{s_2 s_4}}{2} - \int \frac{d^3 P}{(2\pi)^3} \phi_{s_2 s_3}^-(P, k' - P/2) \right. \right. \\ & \left. \left. \phi_{s_3 s_4}^-(P, k' - P/2) \right) v_{s_4}^\dagger(k') \right] v_{s_5}(k) \\ & + \int \frac{d^3 P}{(2\pi)^3} \phi_{s_1 s_2}^-(P, k - P/2) \\ & v_{s_2}^\dagger(k) \chi(P, k - P/2) v_{s_5}(k) \\ & - \int \frac{d^3 P}{(2\pi)^3} u_{s_1}^\dagger(k) \chi(P, k - P/2) u_{s_2}(k) \\ & \left. \left. \phi_{s_2 s_5}(P, k - P/2) \right\}, \quad (88) \end{aligned}$$

where the sum over repeated spin indexes s_i is assumed. These equation can be condensed into,

$$\begin{aligned} E = & u^\dagger \vec{\alpha} \cdot \vec{k} u - \frac{1}{2} \left\{ u^\dagger \int_{k'} V \left(\Lambda^+ - \Lambda^- \right) u \right\}, \quad (89) \\ 0 = & +u^\dagger \vec{\alpha} \cdot \vec{k} v + \left[\int_P \phi^- v^\dagger i \chi v - \int_P u^\dagger i \chi u \phi^- \right] \\ & - \frac{1}{2} u^\dagger \left[\int_{k'} V \left(\Lambda^+ - \Lambda^- \right) \left(1 - 2 \int_P \phi^- \phi^{-\dagger} \right) \right] v. \end{aligned}$$

The couplings of the π to a quark line $u^\dagger \chi u$ and to an antiquark line $v^\dagger \chi v$ have already been calculated. These are derivative couplings (proportional to the momentum) and are negligible in the low P limit. In this model the low P limit dominates the integral in P because for large P the negative energy component ϕ^- of the wave function is almost vanishing. Thus the dominant effect of coupled channels is to multiply the potential term in the mass gap equation by a factor of ,

$$1 - 2 \int_P \phi^- \phi^{-\dagger}. \quad (90)$$

This clearly decreases the term which is the source for the spontaneous breaking of chiral symmetry. Thus the coupled channel effect is to restore partially chiral symmetry.

The signs of the new terms in the mass gap equation are crucial to determine whether the coupled channel effect will increase or decrease the chiral condensation. Because the coupled channel terms introduce in the mass gap equation a new fermion loop it is natural for Dirac Fermions that the coupled channel terms should be affected with a $-$ sign. When the Dirac fermions are translated into Weyl fermions the quarks divide into the species of quarks and antiquarks which have independent field operators and propagators, and the $-$ signs are transferred from the propagator and the loops into the antiquark vertex and the exchange diagrams,

$$: \bar{\psi} \Gamma \psi : \rightarrow b^\dagger \Gamma b, b^\dagger \Gamma d^\dagger, d \Gamma b, -d^\dagger \Gamma d. \quad (91)$$

Loops with a single species still have a $-$ sign but vanish when the integral in the energy is performed, if there is more than one propagator. We find that with Weyl fermions the $-$ sign persists and is due to the quark (antiquark) exchange. This effect is model independent. Only retardation, which was not included here, might perhaps oppose to this negative sign. Thus we may assume quite generally that coupled channels oppose to the breaking of chiral symmetry.

C. Solution of the mass gap equation

In this paper we calculate the minimal contribution of the coupled channels to the mass gap equation. It is not sensible to engage in full feedback computations from the onset, when the formalism is still being explored. We will only include the effect of bare pions in the meson loop. A possible method to compute the coupled channel contributions would be to fold the mass gap equation with a scalar wavefunction of arbitrary parameter α_s . In this case we should recover the coupling of a scalar to a pair of π which was already obtained in eq. (62). This shows that the terms with the coupling of a π to a quark or an antiquark line will cancel. The dominant contribution both for large and small P can then be assumed to be the one with the factor (90). We will now focus on the dominant terms among the coupled channel contributions, We obtain the *momentum* \otimes *spin* coupled channel contribution,

$$\xi = -2 \int \frac{d^3 P}{(2\pi)^3} \phi^-(k + P/2) \phi^-(k + P/2)^\dagger \quad (92)$$

The integrand of eq. (92) was already studied in eqs. (48,53) in the limits,

$$P \rightarrow 0, \quad \phi^- \phi^{-\dagger} \simeq \frac{1}{2} \frac{S^2}{0.08 P}$$

$$P \rightarrow \infty, \quad \phi^- \phi^{-\dagger} \simeq \frac{1}{2} \frac{4}{P^6} \frac{e^{-\frac{(K-P/2)^2}{\alpha_p^2}} - e^{-\frac{(K+P/2)^2}{\alpha_p^2}}}{2 \mathcal{N}_p^2 k P / \alpha_p^2} \quad (93)$$

where the spin factor from $\frac{i\sigma_2}{\sqrt{2}} \frac{-i\sigma_2}{\sqrt{2}}$ is included. For instance for a vanishing quark momentum k the integrand in eq. (92) simplifies to,

$$P \rightarrow 0, \quad 2 \frac{P^2}{2\pi^2} \phi^- \phi^{-\dagger} \simeq 0.63 P$$

$$P \rightarrow \infty, \quad 2 \frac{P^2}{2\pi^2} \phi^- \phi^{-\dagger} \simeq 0.56 (P/2)^{-4.75} e^{-(P/2)^{1.5}}. \quad (94)$$

The integral that leads to ξ is now evaluated with an interpolation between these two limits. We show in Fig. 5 a possible interpolation. because this interpolation is arbitrary, we have to include in the result a theoretical error.

We obtain the *momentum* \otimes *spin* coupled channel contribution,

$$\xi(k) = -(1.1 \pm 0.2) S \quad (95)$$

which turns out to have a shape very close to the function $S = \sin \phi(k)$ which was evaluated at the BCS level.

The dominant coupled channel contribution to the mass gap equation (88) essentially subtracts $2 \int \phi^- \phi^{-\dagger}$ to the 1 of the BCS mass gap equation. The calculation of $\int \phi^- \phi^{-\dagger}$ includes the sum in color and flavor. We estimate that the coupling to the quasi Goldstone bosons, including the momentum, spin, color and flavor contributions yields,

$$\begin{aligned} \xi(k) &\simeq - (1.1 \pm 0.2) S(k) \frac{1}{3} \left(N_f - \frac{1}{N_f} \right) \\ &\simeq (-0.75 \pm 0.3) S(k), \quad N_f = 2 \rightarrow 3. \end{aligned} \quad (96)$$

N_f is the number of almost massless quark flavors which empirically is between 2 and 3. The sign of the coupled channel contribution is opposed to the BCS one (which corresponds to the factor 1), and it reduces the breaking of chiral symmetry. For instance in the BCS case the vacuum energy density can be studied as a function of the quark condensate scale β . It consists in the sum of a kinetic term scaling with β^4 which is positive and an interaction term which scaling with β^{3-n} which is negative, where n is the exponent of the confining potential in a monomial form r^n . In the present model $n = 2$. Then the vacuum energy density has a "Mexican hat" form with the minimum at a finite β , and spontaneous chiral symmetry breaking occurs. In the present case the interaction term decreases because of the coupled channels, and the vacuum with minimum energy density is shifted towards the trivial chiral invariant vacuum.

The mass gap equation can be solved for a coupled channels contribution equal to ξ , when $\xi \geq -1$,

$$0 = u^\dagger \left[\vec{\alpha} \cdot \vec{k} - \frac{1}{2} \int V(\Lambda^+ - \Lambda^-)(1 + \xi) \right] v \quad (97)$$

$$\begin{aligned}
&= u^\dagger \left\{ \vec{\alpha} \cdot \vec{k} + \frac{1}{2} \Delta \left[(S\beta + C\vec{\alpha} \cdot \hat{k})(1 + \xi) \right] \right\} v \\
&= \left[kS - \left(\frac{\varphi''}{2} + \frac{\varphi'}{k} + \frac{SC}{k^2} \right) (1 + \xi) - \xi' \varphi' \right] \vec{\sigma} \cdot \vec{k} i \sigma_2
\end{aligned}$$

The solution φ for $\xi = -0.75 S$ is shown in Fig. 6. In this case and for the same parameter K_0 , the quark condensate is decreased by 90%. We estimate that complete calculations in this model would reduce the quark condensate by 50% to 100%.

We do not include yet the feedback of the new chiral angle φ in the meson wavefunctions ϕ , and in the coupled channel contribution to the mass gap equation $\int \phi^- \phi^{-\dagger}$. This should only be completed in the framework where the coupled mesons are dressed mesons. Nevertheless it is possible to anticipate the coupled channel effects would be reduced. Since the coupled channels oppose to the breaking of chiral symmetry, the variational principle suggests that a reduction of the coupling would both decrease the vacuum energy and increase the breaking of chiral symmetry.

D. A model independent but crude bound for the Decay of the scalar f_0 to a pair of π

It is possible to estimate approximately the relation between the scalar decay and the coupled channel contribution to the mass gap equation. In this sense an upper bound for the decay width of the scalar f_0 to a pair $\pi\pi$ appears naturally. At the same time different models can be tested. The role of the mass gap equation is to insure the vacuum stability, by preventing the generation of scalar mesons directly from the vacuum. If we fold the mass gap equation by the scalar meson amplitude, we get the equation,

$$0 = \underbrace{\triangleleft f_0 \rightrightarrows S_0^{-1} \triangleright}_{(a)} - \underbrace{\triangleleft f_0 \rightrightarrows \pi\pi \triangleright}_{(b)} - \underbrace{\triangleleft f_0 \rightrightarrows \pi\pi \triangleright}_{(c)}, \quad (98)$$

where a model with free quarks would just include (a), the mass gap equation at the BCS level is provided with (b) and the coupled channel effects are summed in (c). The coupled channel term (c) involves directly the form factor for the coupling of a scalar f_0 to a pair of π , which is shown in eq. (62). This also contributes to the pole of a Breit-Wigner meson which is composed by the bare mass M_0 plus the coupled channel contribution which is composed by a real mass shift and an imaginary term. The imaginary component of the mass corresponds to the width,

$$-\frac{i}{2} \Gamma = Im \quad \text{[diagram of a scalar meson decaying into two pions]} + Im \quad \text{[diagram of a scalar meson decaying into two pions with a loop]} \quad (99)$$

The only model dependent term in eq. (98) is precisely the BCS term (b).

In this section we will follow two assumptions which are obeyed by our model and seem natural. Firstly we suppose that the coupled channel terms have the same sign as the S_0^{-1} and thus oppose to the BCS term which produces single handed the dynamical breaking of chiral symmetry. The difference in sign is justified by the extra fermion loop. Secondly we suppose that there is one dominant scale in the model which is present both in the scale of the quark mass, the chiral angle and the quark condensate in one hand, and in the scale of light meson wave functions (including the pion and the scalars) and the coupled channel form factors in the other hand. The connection between these two scales is provided by the Ward Identity, which shows that the π Bethe-Salpeter amplitude for the π is given by the dynamical mass of the quark, and thus by the quark condensate. The scalar meson is also a solution of the same bound State equation with one angular and one spin excitation, and should have approximately the same size. The form factor for the coupling of the scalar f_0 to a pair of π is calculated with an overlap kernel which includes these wave-functions and thus should also reflect the same scale. Thus we suppose that the quark condensate φ , the scalar radial wave-function ϕ and the overlap form factor f can be expressed with the help of the same Gaussian,

$$\sin(\varphi) = e^{\frac{-k^2}{2\beta^2}}, \quad \mathcal{N}\phi = k e^{\frac{-k^2}{2\beta^2}}, \quad f = C e^{\frac{-k^2}{2\beta^2}} \quad (100)$$

where we also suppose that the same coupling f appears in both the mass gap equation and the scalar. In this case we get from the quark condensate, the mass gap and the width, a system of equations,

$$\begin{aligned}
\langle \bar{q}q \rangle &= -6 \int \frac{d^3k}{(2\pi)^3} \sin(\varphi) = -\frac{3}{\pi\sqrt{2\pi}} \beta^3, \\
(a) &= \sqrt{12} \int \frac{d^3k}{(2\pi)^3} \phi^\dagger k \sin(\varphi) = \frac{3}{2\sqrt{\pi\sqrt{\pi}}} \beta^{\frac{5}{2}}, \\
-(c) &= \frac{\sqrt{2}}{\sqrt{6}} \left(N_f - \frac{1}{N_f} \right) \int \frac{d^3p}{(2\pi)^3} f = \frac{N_f - \frac{1}{N_f}}{2\pi\sqrt{6\pi}} \beta^3 \mathcal{C}, \\
-\frac{i}{2} \Gamma &= Im \left[2 \frac{3}{12} \int \frac{d^3p}{(2\pi)^3} f^2 \frac{1}{M_{f_0} - 2\sqrt{p^2 + M_\pi^2} + i\epsilon} \right], \\
\Gamma &= \frac{1}{8\pi} q M_{f_0} C^2 e^{\frac{-q^2}{\beta^2}}, \quad 2q = \sqrt{M_{f_0}^2 - 4M_\pi^2}. \quad (101)
\end{aligned}$$

The color, flavor and spin multiplicity factors are 6 for quarks with fixed flavor, N_f for the number of massless flavors, and $N_f^2 - 1$ for the number of Goldstone bosons. It is sensible to split the strangeness from the isospin, and

to consider that the lowest scalar meson f_0 has a flavor wave-function $\frac{u\bar{u}+d\bar{d}}{\sqrt{2}}$. In Γ there are only two flavors as well since we are calculating the partial decay width into pions. However in the meson loop of term (c) the coupling of f_0 to the mesons K, η should also be considered and in this case the number of flavors N_f ranges from 2 to 3.

We use the physical mass of the pion close to 140 MeV . Other inputs are the f_0 mass, and the partial decay width Γ of the scalar to a pair of π , which lay respectively in the range of $400\text{--}1400 \text{ MeV}$ and $30\text{--}1000 \text{ MeV}$. These wide intervals are necessary to encompass different models where the scalar groundstate could be any of the first three f_0 resonances. The scale β is not directly observable. We find that $\beta \simeq 350 \text{ MeV}$ corresponds to a quark condensate of $(-250 \text{ MeV})^3$ which is not directly observable but is used in most of the literature. The corresponding hadronic size would be smaller than the electromagnetic radius. However the electromagnetic radius might still be reproduced when the vector meson dominance is considered. Yet $\beta \simeq 200 \text{ MeV}$ yields directly a baryon size compatible with the electromagnetic radius. It seems sensible to study both these β scales. We find that,

$$-(c)/(a) = \left[\frac{2}{3} \frac{N_f - N_f^{-1}}{\sqrt{3\pi\sqrt{\pi}}} \right] \sqrt{\beta/q} e^{(q^2/2\beta^2)} \sqrt{\frac{\Gamma}{M_{f_0}}} \quad (102)$$

Where the first factor ranges from .24 to .44 respectively for 2 and 3 light flavors, and .34 seems to be an acceptable value. We show in Fig. 7 the ratio between the new chiral symmetry restoring term $-(c)$ and the free term (a) which was the only chiral symmetry restoring term equal in the BCS case. Due to the equal scale approximation this result should be just regarded as qualitative. See Fig. 1 for the experimentally observed masses and widths.

A large effect is obtained if the scalar f_0 groundstate is the σ with a mass and width of the order of 500 MeV . In this case we find that the mass gap equation is affected with sizeable coupled channel effects, and the parameters used at the BCS level should be reassessed. The interaction term (b) must increase by 50% to 70% in order to maintain the size of the quark condensate. This σ meson is favored by the One Meson Exchange Potentials of nuclear physics. It might also reproduce the $\pi\pi$ phase shifts, with a mass which is interpreted to be in the range $M_{f_0} = 400\text{--}1200 \text{ MeV}$ with a width $\Gamma = 600\text{--}1000 \text{ MeV}$. We estimate that the larger widths and masses in these intervals would most likely exclude the dynamical breaking of chiral symmetry.

In the case that the scalar groundstate is the experimentally confirmed resonance with the mass of $M_{f_0} = 980 \text{ MeV}$ and the partial width to a π pair of $\Gamma = 30 \rightarrow 70 \text{ MeV}$ then we find two different pictures. In the case of large hadrons with $\beta = 200 \text{ MeV}$, the interaction term

(b) must increase by 60% in order to maintain the size of the quark condensate. In the case of small hadrons with $\beta = 350 \text{ MeV}$, term (b) only needs a 20% increase. This picture, with small hadrons, large quark condensate, and low coupled channel effects is most interesting for quark models with chiral symmetry breaking, since the BCS approximation would remain acceptable.

In a different picture are the effective unitarized meson models [4,5] with large nonlinear coupled channel effects. There the scalar groundstate corresponds partly to the $f_0(1370)$ which has a width of the order of 400 MeV . This is acceptable for a β quite larger than 350 MeV . The hadron size β is not an explicit parameter in models [4,5]. But from the momentum cutoffs it is possible to estimate that the mesons are very small which is indeed compatible with a large β .

We find that these pictures are opposite. This criterion assigns a particular size to hadrons for each of the three pictures. From the perspective of quark models a scalar mass $M_{f_0} = 980 \text{ MeV}$ would be more consistent with the vector mass $M_w = 782 \text{ MeV}$, because they are separated by an angular excitation. However at the moment neither of the three pictures can be ruled out.

IV. RESULTS AND CONCLUSION

We developed a general formalism to include both the effects of chiral symmetry breaking and strong hadron-hadron interactions in quark models. This is encouraging since both effects are firmly established in phenomenology. We find new general effects in the mass shifts of the hadron spectrum, the breaking of chiral symmetry, and the scalar meson width. Quantitative results are computed within a particular model.

Concerning real mass shifts we estimate that they are canceled due to the new terms which are introduced by the Ward Identities. This might improve previous [4,5,11] coupled channel calculations where this cancellation was not explicitly included. An overall shift of the hadron spectrum is not expected. In this sense we agree with the results of Geiger and Isgur [30]. Nevertheless mass splittings between states with different quantum numbers are still expected from the boundstate equation. Different theoretical problems that could be reviewed with these new techniques are the contribution of the coupled channels to the hadron spectra, for instance to the interesting η' mass or to the N mass.

Compared with χSB at the BCS level, a new parameter has been identified, which leads to the percentage of coupled channel effects in the mass gap equation. This parameter is related to the width of the scalar meson f_0 and with the size of hadrons. This link can be applied to the study of the decay of scalar meson resonances f_0 in a pair of π . We find that the $\sigma = f_0(600)$ can only be accepted as a candidate for the light strangeless $q\bar{q}$ scalar groundstate if it has a low mass. Even in this case

where χSB survives the coupling of channels, a large 50% reduction of the quark condensate is suggested. The preferred candidate in quark models is the narrow $f_0(980)$. In the case where hadrons are smaller than their electromagnetic radius the effect of coupled channels in the mass gap equation is weak. In this case the BCS approximation is correct for the study of resonances. The $f_0(1370)$ can only be a candidate in the case that the hadronic radius is very small, and would in any case reduce strongly the quark condensate. An experimental measurement of the generic quark radius of light hadrons would suffice to discriminate which of the f_0 resonances corresponds to the light strangeless quark antiquark groundstate.

Accurate calculations were performed in the case where the coupled pair of mesons are accounted as bare mesons, for a class of absolutely confining instantaneous interactions. This model (with a single parameter in the interaction) is in very good agreement with the experiment in what concerns the hadronic spectroscopy, the decays of the vector mesons ρ and Φ , the coupling of a π to a N or Δ and the NN short range interaction [11], moreover it supports that chiral symmetry breaking is very stable in the presence of Nuclear Matter [28]. We find in this model that coupled channels decrease the quark condensate by 50% \rightarrow 100%. This agrees qualitatively with the model independent estimation in the case of $\beta = 200 \text{ MeV}$. We also find in this model that the mass of the light $q\bar{q}$ scalar f_0 meson is close [22] to the experimental mass of the $f_0(980)$, and not to the $f_0(600)$ or the $f_0(1370)$. This apparently indicates a possible solution to the scalar meson puzzle without Deasons, Glueballs or strongly nonlinear coupled channel effects. In this case the attraction which is visible in $\pi\pi$ phase shifts and in the intermediate range NN interactions would need other interpretations [29] than the very wide σ meson. However a complete and exhausting calculation, where the coupled pair of mesons are fully dressed mesons and the feed back from the mass gap equation into the width is included, is necessary to certify within this model that the light $q\bar{q}$ scalar has a mass of the order of 1 GeV and a very narrow width. An interesting feedback from chiral symmetry to coupled channels might occur, and can be understood variationally. Since the scalar-pseudoscalar-pseudoscalar coupling opposes to the breaking of chiral symmetry, it is naturally suppressed. This suppression is selective and is not supposed to occur in other hadronic channels. We estimate that in the final calculation the width of the scalar might decrease by a factor of 2. We would also find interesting to apply these new techniques to other particular quark models [24].

Clearly the wrong result of this model so far was is $f_{\pi t}^{3/4} f_{\pi s}^{1/4}$ which is measurable experimentally but turns out to be [22] only 37% of the measured value. The cure of f_π in this model seems to attract some interest. Physical intuition suggests that f_π should be affected either by relativistic invariance or by the coupled channels. The hope in covariant extensions of the model

turned out to fail since they merely [25] increased f_π in 30%. Now we find that the coupled channels reduce the quark condensate $\langle\bar{\psi}\psi\rangle$. Thus they also reduce f_π rather than increase it, according to the relation of Gell-Mann Oakes and Renner. This indicates that the single parameter which is used in this model for the interaction is insufficient. We think that one should now try to extend it with a different degree of freedom in order to find the correct f_π . Although the use of a different linear or funnel shape did not improve the result, a possible cure may still be searched in the short range quark-quark interaction [25]. This might simplify the model in the sense that the BCS approximation could suffice. For instance, if one would arbitrarily set f_π to the experimental value, then the scalar-pseudoscalar-pseudoscalar coupling at low pseudoscalar momentum P would decrease by a factor of $.37^2 \simeq 0.13$. This would strongly suppress coupled channel effects in both the mass gap equation and in mass shifts of resonances. At the same time the decays could remain correct since they depend on the large P limit.

ACKNOWLEDGMENTS

I am very grateful to Emilio Ribeiro for long discussions and suggestions since 1989 on the pion mass problem in relation with the coupled channels, on the BCS mechanism and on Ward identities. I also acknowledge George Rupp, Jean-Marc Richard, Jack Paton, Robin Stinchcombe, Nils Tornqvist, Vitor Vieira, Pedro Sacramento and Adam Szczepaniak for comments or suggestions.

-
- [1] Review of Particle Physics, Particle Data Group, Phys. Rev. D **54**,1 (1996).
 - [2] J. Weinstein, N. Isgur, Phys. Rev. Lett **48**, 659 (1982); Phys. Rev. D **27**, 588 (1983).
 - [3] see for a recent result on the glueball spectroscopy A. Szczepaniak, E. Swanson, C.-R. Ji and S. Cotanch, Phys. Rev. Lett. **76**, 2011 (1996).
 - [4] E. Van Beveren, T. Rijken, K. Metzger, C. Dullemond, G. Rupp, J. Ribeiro Zeit. Phys. C **30**, 615 ,(1986).
 - [5] N. Törnqvist, M. Roos, Phys. Rev. Lett **76**, 1575, (1996); N. Tornqvist Zeit. Phys. C **68**, 647 (1995).
 - [6] P. Bicudo and J. Ribeiro, Phys. Rev. D **42**, 1611 (1990).
 - [7] J. Bardeen, L. N. Cooper and J. R. Schrieffer, Phys. Rev. **108**, 1175 (1957).
 - [8] Y. Nambu, G. Jona-Lasinio, Phys. Rev. **122**, 345 (1961); **124**, 246 (1961). Any extended of this potential, where nucleons are replaced by quarks, version can also be used.
 - [9] F.T. Hawes and A. G. Williams, Phys. Lett. B **268**, 271 (1991); A. Bashir and M. R. Pennington, Phys. Rev. D **50**, 7679 (1994); H. J. Munczek, Phys. Rev. D **52**, 4736

- (1995); A. Bender, C. D. Roberts, L. V. Smekal, Phys. Lett. B **380**, 7 (1996).
- [10] For a preliminary result on the cancellation of infrared divergences in the π mass, see P. Bicudo, preprint FISIST/5-97/CFIF and hep-ph/9703229 (1997).
- [11] P. Bicudo and J. Ribeiro, Phys. Rev. D **42**, 1635 (1990); P. Bicudo, J. Ribeiro and J. Rodrigues, Phys. Rev. C **52**, 2144 (1995); P. Bicudo and J. Ribeiro, Phys. Rev. C **55**, 834, (1997). P. Bicudo, L. Ferreira, C. Placido and J. Ribeiro, Phys. Rev. C **56**, 670, (1997).
- [12] R. Friedrich and H. Reinhardt, Nucl. Phys. A **549**, 406 (1995); S. Gao, C. Shakin and W.-D. Sun, Phys. Rev. C **53**, 1374 (1996); K. Mitchel and P. Tandy, Phys. Rev. C **55**, 1477 (1997); C. Shakin and W.-D. Sun, Phys. Rev. D **55**, 2874 (1997).
- [13] S. Pepin, F. Stancu, M. Genovese, J. M. Richard, to be published in COMO2, world scientific, preprint nucl-th/9608058.
- [14] A. Thomas and G. Miller, Phys. Rev. D **42**, 288 (1991).
- [15] N. Törnqvist, preprint hep-ph/9612238 (1996).
- [16] J. Schrieffer, "Theory of Superconductivity", W. A. Benjamin (1964);
- [17] S. Adler and A. C. Davis, Nucl. Phys. B **224**, 469 (1984).
- [18] H. Pagels, Phys. Rev. D **14**, 2747 (1976).
- [19] The pseudoscalar $\tilde{\mathcal{F}}\mathcal{F}$ appears naturally in glueball models where the η' is massive [3]. The 't Hooft effective interaction applied to quarks [20] can also simulate this effect. The anomaly may also be present at the coupled channel level, for instance in the $\pi - \rho\rho$ coupling even when one does not include the instanton in the effective quark - quark interaction. In this case coupled channel competes with the instanton for the solution of the $U(1)$ problem [15].
- [20] G. 't Hooft Phys. Rev. Lett. **37**, 8 (1976); Phys. Rev. D **14**, 3432 (1976). The instanton interaction was added to a NJL model in V. Bernard, R. L. Jaffe, U.-G. Meissner, Nucl. Phys. B **308**, 753 (1988).
- [21] Early papers are L. V. Keldysh and Yu. V. Kopaev, Sov. Phys. Solid State **6**, 2219 (1965); L. V. Keldysh and A. N. Kozlov, Sov. Phys. JETP **27**, 521 (1968); P. Nozières, S. Schmitt-Rink, Jour. Low Temp. Phys. **59**, 195 (1985). A recent reference is M. Marini, F. Pistolesi and G. C. Strinati, preprint cond-mat/9703160.
- [22] Y. le Yaouanc, L. Oliver, S. Ono, O. Pene and J.-C. Raynal, Phys. Rev. D **29**, 1233 (1984); Phys. Rev. D **31**, 137 (1985).
- [23] J. E. Villate, D.-S. Liu, J. E. Ribeiro, P. Bicudo, Rev. D **47**, 1145 (1993).
- [24] The papers of NJL [8] have been extended in many different directions, in hundreds of papers and we will only cite a few here which remain in the Euclidean space. See for instance the note in ref. [20]. Finite size boundstates were included with the Global Color Model in R. Cahill and C. Roberts, Phys. Rev. D **32**, 2419 (1985). A sophisticated interaction with a general tensor structure, an almost linear long range and perturbative short range is found in Y. Dai, Z. Huang and D. Liu, Phys. Rev. D **43**, 1717 (1991).
- [25] for Lorentz invariant extensions of these models see, Y. Kalinowsky, L. Kaslun, and V. Pervushin, Phys. Lett. B **231**, 288 (1989); R. Horvat, D. Kekez, D. Klabucar and D. Palle, Phys. Rev. D **43**, 1585 (1991); for theoretical foundations of these models see J. Lagae, Phys. Rev. D **45**, 317 (1992); A. Szczepaniak and E. Swanson, Phys. Rev. D **55**, 3987 (1997).
- [26] P. Bicudo, G. Krein, J. Ribeiro and J. Villate, Phys. Rev. D **45**, 1673 (1992);
- [27] P. Bicudo and J. Ribeiro, Phys. Rev. D **42**, 1625 (1990);
- [28] P. Bicudo Phys. Rev. Lett. **72**, 1600 (1994).
- [29] for a recent substitute to the σ meson in $N - N$ interactions, see F. Wang, G. Wu, L. Teng, and T. Goldman, Phys. Rev. Lett. **69**, 2891 (1992); Phys. Rev. C **53**, 1161 (1996). The $\pi\pi$ overlap interaction with quartic interactions would also need to be reviewed.
- [30] P. Geiger and N. Isgur, Phys. Rev. D **44**, 799 (1991); Phys. Rev. Lett. **67**, 1066 (1991); Phys. Rev. D **47**, 5050 (1993).

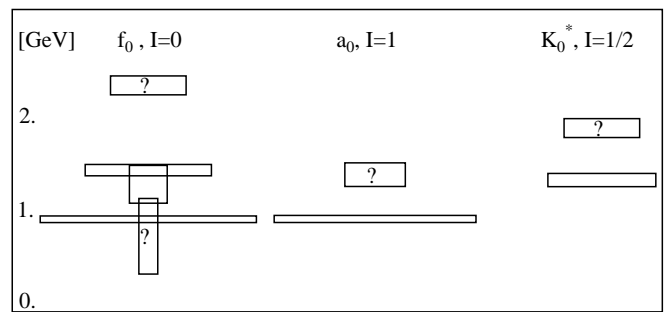


FIG. 1. We show the experimentally observed scalar resonances according to the Review of Particle Properties, and mark the unconfirmed ones with a "?". In a naive quark model, the f_0 would correspond to $\bar{u}u + \bar{d}d$, $\bar{s}s$ mesons (which are not degenerate because the quark s has a clearly larger mass than the quarks u, d). The a_0 and K_0^* channels which would correspond respectively to the degenerate $\bar{u}d, \bar{u}u - \bar{d}d, \bar{d}u$ and to $\bar{u}s, \bar{s}u, \bar{d}s, \bar{s}d$ should show half of the resonances of the f_0 channel.

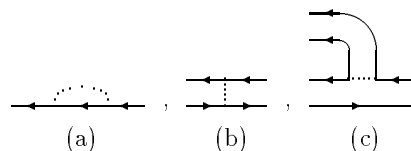


FIG. 2. We show the quartic diagrams which may contribute to the boundstate equation. In the BCS weak coupling approximation the interaction only appears in the self energy or the energy density. Boundstates are studied with diagrams (a) and (b) are already used in NJL which corresponds to a strong coupling BCS. Diagrams (c) which create or annihilate quark-antiquark pairs are only used in what we call beyond BCS.

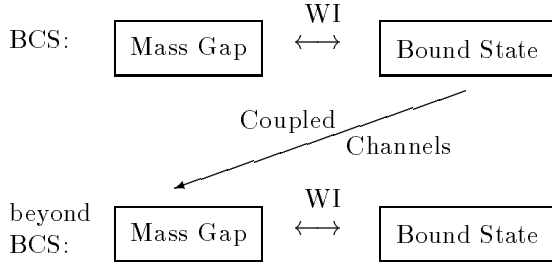


FIG. 3. We illustrate the principle which is followed in this paper to include the coupled channels in the mass gap equation

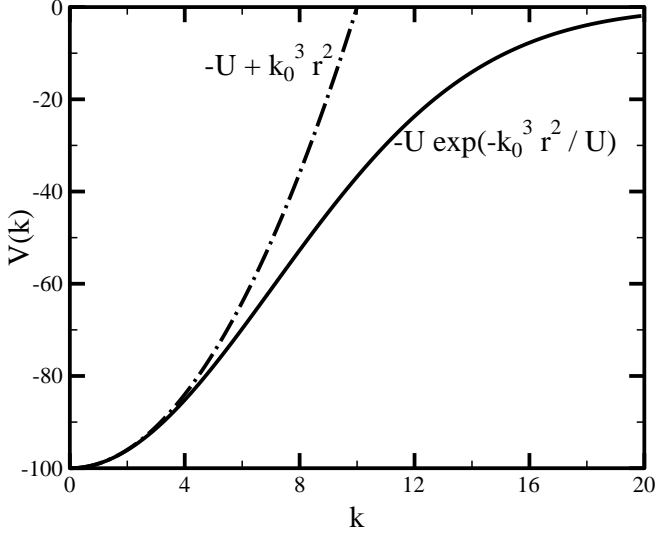


FIG. 4. $-Ue^{-\frac{k_0^3 r^2}{U}}$ is an example of a potential which tends to $-U + k_0^3 r^2$ in the limit of infinite U . We illustrate this in the case where $K_0 = 1$, $U = 100$.

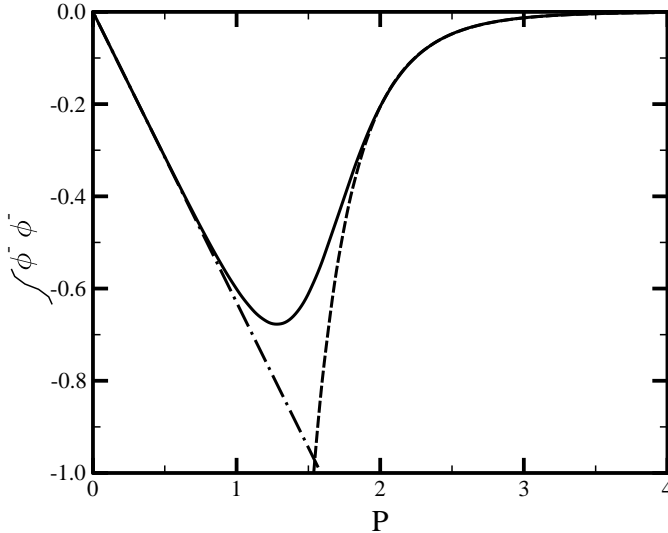


FIG. 5. We show the integrand of the integral $\int dp \frac{-2P^2}{2\pi^2} \phi^-(P, k - P/2) \phi^{-\dagger}(P, k - P/2)$. The dotted line, dashed line, and solid line correspond respectively to the cases where ϕ is obtained in the low P limit, in the high P limit, and with an arbitrary interpolating curve.

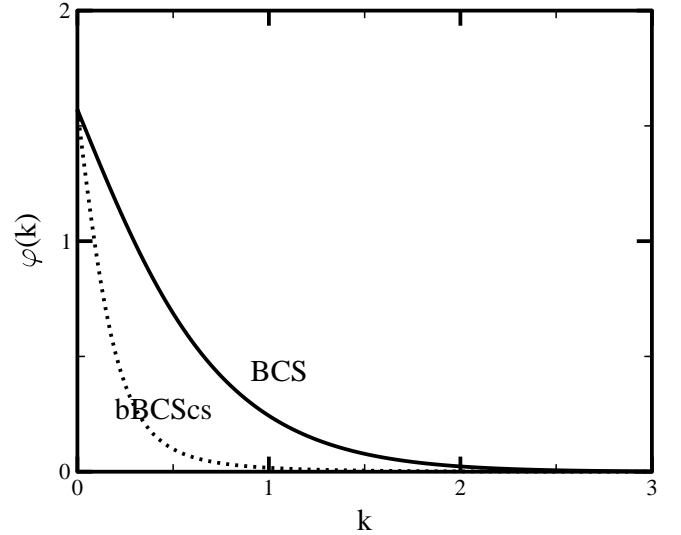


FIG. 6. We show the BCS chiral angle in units of $K_0 = 1$. We also represent with a dotted line the chiral angle that we can obtain within our model going beyond BCS with coupled channels, when $\xi = -800$. In this model we find that coupled channels decrease the quark condensate by 50% to 100%.

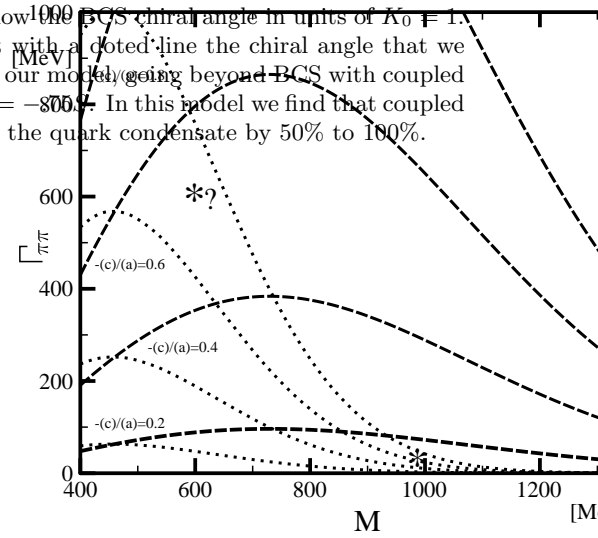


FIG. 7. we show the ratio $\frac{-c(a)}{a}$ of the terms which oppose to chiral symmetry breaking in the coupled channel case versus the BCS case, as a function of the scalar meson mass and as a function of the partial width of the decay of the scalar meson f_0 to a pair of π . The theoretical curves of constant ratio are shown in the cases of 0.2, 0.4, 0.6 and 0.8. The dotted and dashed curves correspond respectively to a scale parameter of $\beta = 200 \text{ MeV}$ and $\beta = 350 \text{ MeV}$. The asterisks correspond to the strongest experimental f_0 candidates to a scalar ll groundstate.